

# Sensitivity physics expected to the measurement of the quartic $WW\gamma\gamma$ couplings at the LHeC and the FCC-he

E. Gürkanli\*,<sup>1</sup> V. Ari†,<sup>2</sup> A. Gutiérrez-Rodríguez‡,<sup>3,4</sup>  
M. A. Hernández-Ruíz§,<sup>5</sup> and M. Köksal¶<sup>6</sup>

<sup>1</sup>*Department of Physics, Sinop University, Turkey.*

<sup>2</sup>*Department of Physics, Ankara University, Turkey.*

<sup>3</sup>*Facultad de Física, Universidad Autónoma de Zacatecas  
Apartado Postal C-580, 98060 Zacatecas, México.*

<sup>4</sup>*Unidad Académica de Estudios Nucleares,  
Universidad Autónoma de Zacatecas, 98060 Zacatecas, México.*

<sup>5</sup>*Unidad Académica de Ciencias Químicas, Universidad Autónoma de Zacatecas  
Apartado Postal C-585, 98060 Zacatecas, México.*

<sup>6</sup>*Department of Optical Engineering, Sivas Cumhuriyet University, 58140, Sivas, Turkey.*

(Dated: August 11, 2020)

---

\* egurkanli@sinop.edu.tr

† vari@science.ankara.edu.tr

‡ alexgu@fisica.uaz.edu.mx

§ mahernan@uaz.edu.mx

¶ mkoksal@cumhuriyet.edu.tr

## Abstract

We explore the physics expected sensitivity at the Large Hadron electron Collider (LHeC) and the Future Circular Collider-hadron electron (FCC-he) to search for the anomalous quartic  $WW\gamma\gamma$  couplings in single  $W$ -boson production in association with a photon. We study the process  $ep \rightarrow e^- \gamma^* p \rightarrow eW\gamma q' X$  via the subprocess  $\gamma^* q \rightarrow W\gamma q'$ . The center-of-mass energies and luminosities of the LHeC are assumed to be  $\sqrt{s} = 1.30, 1.98$  TeV,  $\mathcal{L} = 10 - 100$  fb $^{-1}$  and for the FCC-he  $\sqrt{s} = 3.46, 5.29$  TeV and  $\mathcal{L} = 100 - 1000$  fb $^{-1}$ . Considering these energies and luminosities, we estimate sensitivity measures on the anomalous quartic  $WW\gamma\gamma$  couplings at 95% C.L., which can be an order of magnitude more stringent than the experimental limits reported by ATLAS and CMS Collaborations at the LHC.

PACS numbers: 12.60.-i, 14.70.Fm, 4.70.Bh

Keywords: Models beyond the standard model, W bosons, Quartic gauge boson couplings.

## I. INTRODUCTION

The  $SU(2)_L \times U(1)_Y$  gauge invariant structure of the Standard Model (SM) [1–3] specifies the form and strength of the self-interactions of the vector boson fields, particularly the anomalous Quartic Gauge Couplings (aQGC):  $WW\gamma\gamma$ ,  $WW\gamma Z$ ,  $WWZZ$ ,  $WWWW$ ,  $ZZZZ$ ,  $ZZZ\gamma$ ,  $ZZ\gamma\gamma$ ,  $Z\gamma\gamma\gamma$  and  $\gamma\gamma\gamma\gamma$ . Studying which processes these aQGC could contribute to may yield further confirmation of the non-Abelian gauge structure of the SM or signal the presence of new physics Beyond the SM (BSM) in unprobed energy scales. For instance, the following present and future colliders: the Large Hadron Collider (LHC), the High-Luminosity Large Hadron Collider (HL-LHC), the High-Energy Large Hadron Collider (HE-LHC) [4], the Large Hadron electron Collider (LHeC) [5–8], the Future Circular Collider-hadron electron (FCC-he) [9], the International Linear Collider (ILC) [10], the Compact Linear Collider (CLIC) [11], the Circular Electron Positron Collider (CEPC) [12] and the Future Circular Collider  $e^+e^-$  (FCC-ee) [13]. All of these colliders contemplate in their physics programs the study of the aQGC.

Over the last few years, the aQGC production processes and single- $W$  and double- $W$  production in hadron-hadron, lepton-hadron and lepton-lepton colliders in different collision modes have attracted attention because future colliders with high energies, high luminosities and cleaner environments may allow experimental studies. Such studies are interesting because they allow further independent testing of the SM, the quartic  $WW\gamma\gamma$  vertex can be probed and the Higgs boson plays an important role in  $WW$  channel.

In this paper, we are interested in estimating sensitivity measures in the aQGC  $f_{M,i}$  and  $f_{T,i}$  with  $i = 0, 1, 2, \dots, 7$  for the possible energies and luminosities of the LHeC and the FCC-he in its different stages, i.e.,  $\sqrt{s} = 1.30$  TeV, 1.98 TeV,  $\mathcal{L} = 10$  fb $^{-1}$ , 30 fb $^{-1}$ , 50 fb $^{-1}$ , 100 fb $^{-1}$  and  $\sqrt{s} = 3.46$  TeV, 5.29 TeV,  $\mathcal{L} = 100$  fb $^{-1}$ , 300 fb $^{-1}$ , 500 fb $^{-1}$ , 1000 fb $^{-1}$ , respectively. As shown in Figs. 1 and 2, there are 13 Feynman diagrams at the tree level contributing to the process  $ep \rightarrow e^- \gamma^* p \rightarrow eW\gamma q' X$  via the subprocess  $\gamma^* q \rightarrow W\gamma q'$ , where  $q = u, c, \bar{d}, \bar{s}$  and  $q' = d, s, \bar{u}, \bar{c}$ .

For an experimental and phenomenological review of the measurement evolution of the limits on the aQGC in the context of previous, present and future colliders, such as the LEP at the CERN [14–17], D0 and CDF at the Tevatron [18, 19], ATLAS and CMS at the LHC [20, 21] and in the post-LHC era as the LHeC and the FCC-he [22, 23], the ILC, the CLIC,

the CEPC and the FCC-ee, see Refs. [24–57], as well as Table I of Ref. [23].

This paper describes searches for the sensitivity physics expected to the measurement of the  $WW\gamma\gamma$  aQGC at the LHeC and the FCC-he using the process  $ep \rightarrow e^-\gamma^*p \rightarrow eW\gamma q'X$ . In Section II, we briefly describe the theoretical aspects of the operators in our effective Lagrangian and in Section III, we derive the bounds for the aQGC at the LHeC and the FCC-he. We summarize our conclusions in Section IV.

## II. BRIEF REVIEW OF THE THEORETICAL ASPECTS

The Effective Field Theory (EFT) approach is very useful in the absence of a specific model of new physics. An EFT parameterizes the low-energy effects of the new physics to be found at higher energies in a model-independent way.

With this approach, we start from an EFT to probe model-independent sensitivity measures on  $W^+W^-\gamma\gamma$  quartic gauge boson vertex. The EFT approach is the natural way to extend the SM such that the gauge symmetries are respected. In addition, the EFT is general enough to capture any BSM physics and provides guidance as to the most likely place to see the effects of new physics.

The measurement of the  $WW\gamma\gamma$  couplings can be made quantitative by introducing a more general  $WW\gamma\gamma$  vertex. For our discussion of phenomenological sensitivities in Section III, we shall use the phenomenological effective Lagrangian which comes from several  $SU(2)_L \times U(1)_Y$  invariant dimension-8 effective operators [58]:

$$\mathcal{L}_{eff} = \sum_{i=1}^2 \frac{f_{S,i}}{\Lambda^4} O_{S,i} + \sum_{i=0}^9 \frac{f_{T,i}}{\Lambda^4} O_{T,i} + \sum_{i=0}^7 \frac{f_{M,i}}{\Lambda^4} O_{M,i}. \quad (1)$$

In this equation, the indices S, T and M of the couplings and operators represent three classes of genuine aQGC operators [57]. The  $f_{T,i}/\Lambda^4$  associated operators characterize the effect of new physics on the scattering of transversely polarized vector bosons, and  $f_{M,i}/\Lambda^4$  includes mixed transverse and longitudinal scatterings. A list of these operators is given below.

- i) First class of independent scalar operators:

$$O_{S,0} = [(D_\mu \Phi)^\dagger (D_\nu \Phi)] \times [(D^\mu \Phi)^\dagger (D^\nu \Phi)], \quad (2)$$

$$O_{S,1} = [(D_\mu \Phi)^\dagger (D^\mu \Phi)] \times [(D_\nu \Phi)^\dagger (D^\nu \Phi)]. \quad (3)$$

ii) Second class of independent mixed operators:

$$O_{M,0} = Tr[W_{\mu\nu} W^{\mu\nu}] \times [(D_\beta \Phi)^\dagger (D^\beta \Phi)], \quad (4)$$

$$O_{M,1} = Tr[W_{\mu\nu} W^{\nu\beta}] \times [(D_\beta \Phi)^\dagger (D^\mu \Phi)], \quad (5)$$

$$O_{M,2} = [B_{\mu\nu} B^{\mu\nu}] \times [(D_\beta \Phi)^\dagger (D^\beta \Phi)], \quad (6)$$

$$O_{M,3} = [B_{\mu\nu} B^{\nu\beta}] \times [(D_\beta \Phi)^\dagger (D^\mu \Phi)], \quad (7)$$

$$O_{M,4} = [(D_\mu \Phi)^\dagger W_{\beta\nu} (D^\mu \Phi)] \times B^{\beta\nu}, \quad (8)$$

$$O_{M,5} = [(D_\mu \Phi)^\dagger W_{\beta\nu} (D^\nu \Phi)] \times B^{\beta\mu}, \quad (9)$$

$$O_{M,6} = [(D_\mu \Phi)^\dagger W_{\beta\nu} W^{\beta\nu} (D^\mu \Phi)], \quad (10)$$

$$O_{M,7} = [(D_\mu \Phi)^\dagger W_{\beta\nu} W^{\beta\mu} (D^\nu \Phi)]. \quad (11)$$

ii) Third class of independent transverse operators:

$$O_{T,0} = Tr[W_{\mu\nu} W^{\mu\nu}] \times Tr[W_{\alpha\beta} W^{\alpha\beta}], \quad (12)$$

$$O_{T,1} = Tr[W_{\alpha\nu} W^{\mu\beta}] \times Tr[W_{\mu\beta} W^{\alpha\nu}], \quad (13)$$

$$O_{T,2} = Tr[W_{\alpha\mu} W^{\mu\beta}] \times Tr[W_{\beta\nu} W^{\nu\alpha}], \quad (14)$$

$$O_{T,5} = Tr[W_{\mu\nu} W^{\mu\nu}] \times B_{\alpha\beta} B^{\alpha\beta}, \quad (15)$$

$$O_{T,6} = Tr[W_{\alpha\nu} W^{\mu\beta}] \times B_{\mu\beta} B^{\alpha\nu}, \quad (16)$$

$$O_{T,7} = Tr[W_{\alpha\mu} W^{\mu\beta}] \times B_{\beta\nu} B^{\nu\alpha}, \quad (17)$$

$$O_{T,8} = B_{\mu\nu} B^{\mu\nu} B_{\alpha\beta} B^{\alpha\beta}, \quad (18)$$

$$O_{T,9} = B_{\alpha\mu} B^{\mu\beta} B_{\beta\nu} B^{\nu\alpha}. \quad (19)$$

In the operators (2)-(19)  $D_\mu$  is the covariant derivative,  $\Phi$  denotes the Higgs double field and  $B^{\mu\nu}$ ,  $W^{\mu\nu}$  are the field strength tensors. The  $O_{S,0}$  and  $O_{S,1}$  operators given by Eqs. (2) and (3) contain the quartic  $W^+W^-W^+W^-$ ,  $W^+W^-ZZ$  and  $ZZZZ$  couplings, which do not concern us here. An exhaustive study on the mechanism to build the dimension-8 operators corresponding to the aQGC is presented in Refs. [32, 40, 41, 56–58].

### III. CROSS SECTION MEASUREMENTS AT THE LHEC AND THE FCC-HE

The phenomenological investigations at  $ep$  colliders generally contain usual deep inelastic scattering reactions where the colliding proton dissociates into partons. These reactions have been extensively examined in the literature, but exclusive and semi-elastic processes that are  $\gamma^*\gamma^*$  and  $\gamma^*p$  have been studied much less. These exclusive and semi-elastic processes have simpler final states with respect to  $ep$  processes and thus compensate for the advantages of  $ep$  processes such as having a higher center-of-mass energy and luminosity. Here,  $\gamma^*p$  processes have effective luminosity and much higher energy compared to  $\gamma^*\gamma^*$  process. This may be significant because of the high energy dependencies of the cross-sections containing the new physics parameters and for this reason,  $\gamma^*p$  processes are expected to have a high sensitivity to the aQGC.

$\gamma^*p$  processes can be discerned from usual deep inelastic scattering processes by means of two experimental signatures [59]. The first signature is the forward large rapidity gap [60–63]. Quasi-real photons have a low virtuality and scatter with small angles from the beam pipe. Since the transverse momentum carried by a quasi-real photon is small, photon-emitting electrons should also be scattered with small angles and exit the central detector without being detected. This causes a decreased energy deposit in the corresponding forward region. As a result, one of the forward regions of the central detector has a significant lack of energy. This defines the forward large-rapidity gap, and usual  $ep$  deep inelastic processes can be rejected by applying a selection cut on this quantity. The second experimental signature is provided by the forward detectors [64–66] which are capable of detecting particles with a large pseudorapidity. When a photon-emitting electron is scattered with a large pseudorapidity, it exceeds the pseudorapidity coverage of the central detectors. In these processes, the electron can be detected by the forward detectors which provides a distinctive signal for  $\gamma^*p$  processes. In this context, LHeC Collaboration has a program of forward physics with extra detectors located in a region between a few tens up to several hundreds of meters from the interaction point [66].

In this section, the cross section of the  $ep \rightarrow e^- \gamma^* p \rightarrow eW \gamma q' X$  signal is evaluated for the center-of-mass energies and luminosities of the LHeC and the FCC-he with their respective energies and luminosities  $\sqrt{s} = 1.30, 1.98$  TeV,  $\mathcal{L} = 10 - 100$  fb $^{-1}$  and  $\sqrt{s} = 3.46, 5.29$  TeV,  $\mathcal{L} = 100 - 1000$  fb $^{-1}$ . For  $ep \rightarrow e^- \gamma^* p \rightarrow eW \gamma q' X$  signal, we consider leptonic and hadronic

decays of the  $W$ -boson;  $W \rightarrow \nu_l l$ ,  $W \rightarrow qq'$  with  $\nu_l = \nu_e, \nu_\mu$ ,  $l = e^-, \mu$  and  $q = u, c, \bar{d}, \bar{s}$ ,  $q' = d, s, \bar{u}, \bar{c}$ , respectively.

Formally, the  $ep \rightarrow e^- \gamma^* p \rightarrow eW\gamma q'X$  cross section can be split into three parts:

$$\begin{aligned} \sigma_{tot} \left( \sqrt{s}, \frac{f_{M,i}}{\Lambda^4}, \frac{f_{T,i}}{\Lambda^4} \right) &= \sigma_{BSM} \left( \sqrt{s}, \frac{f_{M,i}^2}{\Lambda^8}, \frac{f_{T,i}^2}{\Lambda^8}, \frac{f_{M,i} f_{T,i}}{\Lambda^4 \Lambda^4} \right) + \sigma_{int} \left( \sqrt{s}, \frac{f_{M,i}}{\Lambda^4}, \frac{f_{T,i}}{\Lambda^4} \right) \\ &+ \sigma_{SM}(\sqrt{s}), \quad i = 0, \dots, 7, \end{aligned} \quad (20)$$

where  $\sigma_{BSM}$  is the contribution due to BSM physics, which in our case comes from the anomalous vertex  $WW\gamma\gamma$ .  $\sigma_{int}$  is the interference term between SM and the new physics contribution and  $\sigma_{SM}$  is the SM prediction, respectively.

To optimize the measurement of the electroweak-induced  $eW\gamma q'X$  signal and improve the electroweak signal significance, we further consider selections on the following variables to suppress backgrounds. Following is a summary of the baseline selection criteria for the kinematics cuts on the final state particles:

**i) Cuts-0:** Selected cuts for the  $p_T$ :

- $p_T^q > 20$  GeV (minimum  $p_T$  for the jets), (21)

- $p_T^\gamma > 10$  GeV (minimum  $p_T$  for the photons), (22)

- $p_T^l > 10$  GeV (minimum  $p_T$  for the charged leptons). (23)

**ii) Cuts-1:** Selected cuts for the  $\eta$ :

- $|\eta_q| < 5$  (maximum rapidity for the jets), (24)

- $|\eta_\gamma| < 2.5$  (maximum rapidity for the photons), (25)

- $|\eta_l| < 2.5$  (maximum rapidity for the charged leptons). (26)

**iii) Cuts-2:** Selected cuts for the  $\Delta R$ :

- $\Delta R_{qq} = 0.4$  (minimum distance between jets), (27)

- $\Delta R_{ll} = 0.4$  (minimum distance between leptons), (28)

- $\Delta R_{\gamma q} = 0.4$  (minimum distance between  $\gamma$  and jet), (29)

- $\Delta R_{ql} = 0.4$  (minimum distance between jet and lepton), (30)

- $\Delta R_{\gamma l} = 0.4$  (minimum distance between  $\gamma$  and lepton). (31)

As we mentioned above, the kinematic cuts given by Eqs. (21)-(31) are applied to reduce the background and to reach higher expected significance for the possible aQGC signal in the process  $ep \rightarrow e^- \gamma^* p \rightarrow eW\gamma q' X$ . The sensitivities are investigated using the Monte Carlo simulations with a leading order in MadGraph5\_aMC@NLO [67]. The operators described in Eqs. (4)-(19) are implemented into MadGraph5\_aMC@NLO through Feynrules package [68] as a Universal FeynRules Output (UFO) module [69].

The future lepton-hadron colliders, such as the LHeC and the FCC-he can be operated as  $\gamma^* p$  colliders, in this case the emitted quasi-real photon  $\gamma^*$  is scattered with small angles from the beam pipe of  $e^-$  [70–75]. These processes can be described by the Equivalent Photon Approximation (EPA) [73, 76, 77], using the Weizsacker-Williams Approximation. The main idea of EPA is that the electromagnetic interaction of an electron with the complicated field of the proton bunch is replaced by a simpler Compton scattering of this proton with the flux of EPA generated by the electron bunch. For our case, the schematic diagram for the process  $ep \rightarrow e^- \gamma^* p \rightarrow eW\gamma q' X$  is given by Fig. 1 and the Feynman diagrams of the subprocess  $\gamma^* q \rightarrow W\gamma q'$  are shown in Fig. 2. In this context, the spectrum of EPA photons is given by [73, 78]:

$$f_{\gamma_1^*}(x_1) = \frac{\alpha}{\pi E_e} \left\{ \left[ \frac{1 - x_1 + x_1^2/2}{x_1} \right] \log\left(\frac{Q_{max}^2}{Q_{min}^2}\right) - \frac{m_e^2 x_1}{Q_{min}^2} \left( 1 - \frac{Q_{min}^2}{Q_{max}^2} \right) - \frac{1}{x_1} \left[ 1 - \frac{x_1}{2} \right]^2 \log\left(\frac{x_1^2 E_e^2 + Q_{max}^2}{x_1^2 E_e^2 + Q_{min}^2}\right) \right\} \quad (32)$$

where  $x_1 = E_{\gamma_1^*}/E_e$  and  $Q_{max}^2$  is the maximum photon virtuality. The minimum value of  $Q_{min}^2$  is:

$$Q_{min}^2 = \frac{m_e^2 x_1^2}{1 - x_1}. \quad (33)$$



Using all of these tools, the total cross sections (see Eq. (20)) of the  $ep \rightarrow e^- \gamma^* p \rightarrow eW\gamma q'X$  signal at the LHeC and the FCC-he are determined by:

$$\sigma(ep \rightarrow eW\gamma q'X) = \int f_{\gamma^*}(x) \hat{\sigma}(\gamma^* q \rightarrow W\gamma q') dx. \quad (34)$$

The total cross section of the process  $ep \rightarrow e^- \gamma^* p \rightarrow eW\gamma q'X$ , i.e.,  $\sigma(f_{M,i}/\Lambda^4, f_{T,i}/\Lambda^4, \sqrt{s})$  as a function of  $f_{M,i}/\Lambda^4$  and  $f_{T,i}/\Lambda^4$  with  $i = 0, 1, 2, \dots, 7$  for the energies of the LHeC with  $\sqrt{s} = 1.30$  TeV, 1.98 TeV and the FCC-he with  $\sqrt{s} = 3.46$  TeV, 5.29 TeV are reported in a region defined by the kinematics cuts given in Eqs. (21)-(31).

Cross sections of the process  $ep \rightarrow e^- \gamma^* p \rightarrow eW\gamma q'X$  as a function of aQGC  $f_{M,i}/\Lambda^4$  ( $f_{T,i}/\Lambda^4$ ) are given in Figs. (3)-(10). For evaluation of the total cross sections, the leptonic and hadronic decays of the  $W$ -boson in the final state are considered. The total cross sections for each coupling are evaluated while fixing the other couplings to zero.

The corresponding expected cross sections after acceptance cuts for the process  $ep \rightarrow e^- \gamma^* p \rightarrow eW\gamma q'X$  give the value  $\sigma(f_{T,6}/\Lambda^4, \sqrt{s}) \simeq 10^5$  pb for  $|f_{T,6}/\Lambda^4| = 1 \times 10^{-8}$  GeV $^{-4}$  with the hadronic decay channel of the  $W$ -boson. The cross section is  $\sigma(f_{T,6}/\Lambda^4, \sqrt{s}) \simeq 10^4$  pb for the leptonic decay channel of the  $W$ -boson in the final state.

In Tables I and II, we illustrate the total cross sections in the fiducial region given by Eqs. (21)-(31) for the process  $ep \rightarrow e^- \gamma^* p \rightarrow eW\gamma q'X$  with the different  $f_{M,i}/\Lambda^4$  and  $f_{T,i}/\Lambda^4$  couplings, and for the future energies of the LHeC and the FCC-he.

From Figs. 3-10 and Tables I and II, it is clear that the cross section projects a greater dependence with respect to the  $f_{T,6}/\Lambda^4$  and  $f_{T,5}/\Lambda^4$  couplings than the  $f_{M,7}/\Lambda^4$ ,  $f_{M,0}/\Lambda^4$ ,  $f_{M,1}/\Lambda^4$ , etc.. There is also a difference in the measured cross section of up to an order of magnitude between the leptonic and hadronic cases. The cross sections are evaluated in a region defined by the kinematic cuts given by Eqs. (21)-(31).

Table III shows the effects of cuts on the cross-section values of SM and some aQGC. As mentioned above, the kinematic cuts given by Eqs. (21)-(31) are applied to reduce the background and to reach higher expected significance for the possible aQGC signal in the process  $ep \rightarrow e^- \gamma^* p \rightarrow eW\gamma q'X$ . To compare the SM cross section and the total cross sections, we have taken the values of the couplings as  $5 \times 10^{-10}$  GeV $^{-4}$  for center-of-mass energy of 1.98 TeV and  $5 \times 10^{-11}$  GeV $^{-4}$  for center-of-mass energy of 5.29 TeV. For example, regarding the effect of cuts at 5.29 TeV for hadronic decay process, after Cut-0 set is applied,

the cut efficiency is about 4% for the SM background which has the same final state with signal and after applying Cut-1 and Cut-2 sets, the efficiency is reduced by 75%. After the cuts are selected, the SM cross section is more suppressed with respect to the cross sections including the aQGC. Consequently, sensitivities are better when cuts are applied.

In summary, the  $ep \rightarrow e^- \gamma^* p \rightarrow eW\gamma q' X$  cross section in the presence of anomalous couplings increases rapidly with the electron-proton increasing center-of-mass energy.

#### IV. $\chi^2$ ANALYSIS AND SENSITIVITY MEASURES ON THE AQGC $f_{M,i}/\Lambda^4$ AND $f_{T,i}/\Lambda^4$ AT THE LHEC AND THE FCC-HE

We perform  $\chi^2$  analysis to obtain the sensitivity measures on the anomalous  $f_{M,i}/\Lambda^4$  and  $f_{T,i}/\Lambda^4$  couplings.  $\chi^2$  is defined as follows:

$$\chi^2(f_{M,i}/\Lambda^4, f_{T,i}/\Lambda^4) = \left( \frac{\sigma_{SM}(\sqrt{s}) - \sigma_{BSM}(\sqrt{s}, f_{M,i}/\Lambda^4, f_{T,i}/\Lambda^4)}{\sigma_{SM}\delta_{st}} \right)^2, \quad (35)$$

where  $\sigma_{SM}(\sqrt{s})$  is the cross section of the SM and  $\sigma_{BSM}(\sqrt{s}, f_{M,i}/\Lambda^4, f_{T,i}/\Lambda^4)$  is the BSM cross section.  $\delta_{st} = \frac{1}{\sqrt{N_{SM}}}$  is the statistical error and  $N_{SM}$  is the number of events:

$$N_{SM} = \mathcal{L}_{int} \times \sigma_{SM}. \quad (36)$$

Here, we assume the integrated luminosities  $\mathcal{L}_{int} = 10 - 100 \text{ fb}^{-1}$  for the LHeC and  $\mathcal{L}_{int} = 100 - 1000 \text{ fb}^{-1}$  for the FCC-he.

Tables IV and V summarize all sensitivity measures on the dimension-8 aQGC obtained from  $ep \rightarrow e^- \gamma^* p \rightarrow eW\gamma q' X$  data with the leptonic decay of the  $W$ -boson in the final state at center-of-mass energies of  $\sqrt{s} = 1.30, 1.98 \text{ TeV}$  at the LHeC and  $\sqrt{s} = 3.46, 5.29 \text{ TeV}$  at the FCC-he. For these sensitivity measures, all parameters except the one shown are fixed to zero. The results for leptonic final state at  $\sqrt{s} = 3.46 \text{ TeV}$  and  $\sqrt{s} = 5.29 \text{ TeV}$  given in Table V are better values compared to those obtained for the  $\sqrt{s} = 1.30 \text{ TeV}$  and  $\sqrt{s} = 1.98 \text{ TeV}$  presented in Table IV. A similar behaviour can be seen for the hadronic decay of  $W$ -boson given in Tables VI-VII. The sensitivity measures of  $f_{T6}/\Lambda^4 = [-1.10; 1.60] \text{ TeV}^{-4}$  with  $\sqrt{s} = 3.46 \text{ TeV}$  and  $f_{T6}/\Lambda^4 = [-4.37; 5.51] \times 10^{-1} \text{ TeV}^{-4}$  with  $\sqrt{s} = 5.29 \text{ TeV}$  in Table VII are the most stringent. These sensitivity measures are also approximately an order of

magnitude more stringent than those obtained at the LHeC and the FCC-he through the main  $ep \rightarrow e^- \gamma^* p \rightarrow eW \gamma q' X$  reaction. [22, 23].

Table VIII illustrates sensitivity measures on aQGC at the 95% C. L. via  $ep \rightarrow e^- \gamma^* p \rightarrow eW \gamma q' X$  with the EPA for various  $Q_{max}$  values with  $\sqrt{s} = 5.29$  TeV at the FCC-he. The EPA factorize the dependence on virtuality of the photon from the cross-section of the photon-induced process ( $\gamma^* \gamma^*$  and  $\gamma^* p$  collisions) to the equivalent photon flux. However,  $Q_{max}$  dependence of new physics parameters has also been studied in the literature. Ref. [79] has examined  $Q_{max}$  dependence of the cross sections with the EPA for the process  $pp \rightarrow p \gamma^* \gamma^* p \rightarrow p \tau^+ \tau^- p$  without anomalous couplings of tau lepton. They found that the cross sections for  $Q_{max} = (1 - 2)$  GeV do not appreciably change. In addition, the cross sections of the process  $ee \rightarrow e \gamma^* \gamma^* e \rightarrow ee \tau \tau$  at the CLIC for values of  $Q_{max} = (1.41 - 8)$  GeV are obtained in Ref. [80]. The potential of the process  $ep \rightarrow e \gamma^* \gamma^* p \rightarrow e \tau^- \tau^+ p$  at the LHeC and the FCC-he to examine non-standard  $\tau^- \tau^+ \gamma$  coupling in a model independent way by means of the effective Lagrangian approach is investigated in Ref. [81]. In that study,  $Q_{max} = 100$  GeV is assumed and in our case, we consider the maximum photon virtuality  $Q_{max} = 100$  GeV, where this value is the default value in MadGraph5\_aMC@NLO. We calculate the  $Q_{max}$  dependency on the aQGC for the highest center-of-mass energy. In Table VIII, sensitivity measures on aQGC at the 95% C.L. via the process  $ep \rightarrow e \gamma^* p \rightarrow eW \gamma q' X$  for the hadronic decay of  $W$ -boson for  $\mathcal{L} = 1000 \text{ fb}^{-1}$ ,  $\sqrt{s} = 5.29$  TeV and  $Q_{max} = 1.41, 8$  GeV are obtained. We conclude that  $Q_{max}$  dependence on the aQGC does not significantly change.

We now compare our findings with the other results in the literature which used different cuts and different channels. In Ref. [22], a detailed study of the LHeC and the FCC-he sensitivity to the anomalous  $f_{M,i}/\Lambda^4$  and  $f_{T,i}/\Lambda^4$  couplings in  $\nu_e \gamma \gamma q$  production was carried out. Using a  $\chi^2$  analysis and kinematic cuts for the final state particles in  $\nu_e \gamma \gamma q$  production, they obtained limits on the thirteen different anomalous couplings arising from dimension-8 operators. In Ref. [23], limits were obtained from diboson production at both the LHeC and the FCC-he and on the anomalous  $f_{M,i}/\Lambda^4$  and  $f_{T,i}/\Lambda^4$  couplings considering the process  $e^- p \rightarrow e^- \gamma^* \gamma^* p \rightarrow e^- W^+ W^- p$  with the subprocess  $\gamma^* \gamma^* \rightarrow W^+ W^-$ . These limits are weaker by about a factor of 3 or 5 and up to an order of magnitude than our results. CMS Collaboration [82, 83] at the LHC with  $\sqrt{s} = 8$  TeV and to an integrated luminosity of  $19.7 \text{ fb}^{-1}$  searches for exclusive or quasi-exclusive  $WW$  production via the

signal topology  $pp \rightarrow p^*W^+W^-p^*$  where the  $p^*$  indicates that the final state protons either remain intact (exclusive or elastic production), or dissociate into an undetected system (quasi-exclusive or proton dissociation production). Their research is translated into upper limits on the aQGC operators  $f_{M,0,1,2,3}/\Lambda^4$  (dimension-8). From its investigations, CMS Collaboration measures the electroweak-induced production of  $W$  and two jets, where the  $W$  boson decays leptonically, and experimental limits on aQGC  $f_{M,0-7}/\Lambda^4$ ,  $f_{T,0-2,5-7}/\Lambda^4$  are set at 95% C.L.[82, 83]. On the other hand, ATLAS Collaboration at the LHC studied the production of  $WV\gamma$  events in  $e\nu\mu\nu\gamma$ ,  $e\nu qq\gamma$  and  $\mu\nu qq\gamma$  final states with  $\mathcal{L}_{int} = 20.2 \text{ fb}^{-1}$  of proton-proton collisions with  $\sqrt{s} = 8 \text{ TeV}$  [21].

## V. CONCLUSIONS

The calculations on the production cross section in this paper are derived for the  $eW\gamma q'X$  final states at the LHeC with center-of-mass energies  $\sqrt{s} = 1.30, 1.98 \text{ TeV}$  and the FCC-he with  $\sqrt{s} = 3.46, 5.29 \text{ TeV}$  in the fiducial regions given by Eqs. (21)-(31). Our results are summarized through Figs. 3-10 and in Tables I-III. Furthermore, we show individual upper sensitivity measures obtained for the aQGC  $f_{M,0-5,7}/\Lambda^4$  and  $f_{T,0-2,5-7}/\Lambda^4$  at 95% C.L. both at leptonic and hadronic decay channel of the  $W$ -boson in Tables IV-VIII. As can be seen in the results, the process gives strong constraints on aQGC sensitivity measures at high energy region and high luminosities.

In conclusion, we explore the phenomenological aspects of the anomalous  $WW\gamma\gamma$  couplings via the process  $ep \rightarrow e^-\gamma^*p \rightarrow eW\gamma q'X$  at the LHeC and the FCC-he. These couplings are defined through a phenomenological effective Lagrangian. The major goal of these measurements will be the confirmation of the new physics BSM. If the energy scale of the new physics responsible for the non-standard gauge boson couplings  $f_{M,i}/\Lambda^4$  and  $f_{T,i}/\Lambda^4$  is the center-of-mass energy of 5.29 TeV and the integrated luminosity of  $1000 \text{ fb}^{-1}$ , these couplings are expected to be no larger than  $\mathcal{O}(10^{-1})$ . Our results, as well as our expectations, indicate that with cleaner environments, appropriate fiducial regions, high energies and high luminosities for future colliders will be possible to obtain stronger upper sensitivity measures on the anomalous  $WW\gamma\gamma$  couplings.

TABLE I: Summary of the total cross-sections of the process  $ep \rightarrow e^- \gamma^* p \rightarrow eW\gamma q' X$  for  $\sqrt{s} = 1.30, 1.98$  TeV at the LHeC and  $\sqrt{s} = 3.46, 5.29$  TeV at the FCC-he depending on thirteen anomalous couplings obtained by dimension-8 operators. The total cross-sections for each coupling are calculated with the values of  $1 \times 10^{-8}$  GeV $^{-4}$  and  $5 \times 10^{-9}$  GeV $^{-4}$  at the LHeC and the FCC-he, respectively.

$\sigma(ep \rightarrow e^- \gamma^* p \rightarrow eW\gamma q' X)$ (pb)				
	LHeC		FCC-he	
	Leptonic channel		Leptonic channel	
SM	$7.27 \times 10^{-3}$	$2.18 \times 10^{-2}$	$2.27 \times 10^{-2}$	$6.38 \times 10^{-2}$
Couplings	$\sqrt{s} = 1.30$ TeV	$\sqrt{s} = 1.98$ TeV	$\sqrt{s} = 3.46$ TeV	$\sqrt{s} = 5.29$ TeV
$f_{M0}/\Lambda^4$	$2.29 \times 10^{-2}$	$3.98 \times 10^{-1}$	$7.40 \times 10^{-2}$	2.80
$f_{M1}/\Lambda^4$	$1.66 \times 10^{-2}$	$2.29 \times 10^{-1}$	$6.30 \times 10^{-2}$	2.07
$f_{M2}/\Lambda^4$	$6.79 \times 10^{-1}$	$1.62 \times 10^1$	2.29	$1.17 \times 10^2$
$f_{M3}/\Lambda^4$	$4.47 \times 10^{-1}$	9.14	1.83	$8.61 \times 10^1$
$f_{M4}/\Lambda^4$	$5.84 \times 10^{-2}$	1.25	$1.94 \times 10^{-1}$	9.00
$f_{M5}/\Lambda^4$	$4.35 \times 10^{-2}$	$7.27 \times 10^{-1}$	$1.70 \times 10^{-1}$	6.70
$f_{M7}/\Lambda^4$	$1.05 \times 10^{-2}$	$7.69 \times 10^{-2}$	$3.29 \times 10^{-2}$	$5.71 \times 10^{-1}$
$f_{T0}/\Lambda^4$	$9.55 \times 10^{-1}$	$3.59 \times 10^1$	5.39	$5.85 \times 10^2$
$f_{T1}/\Lambda^4$	2.61	$8.10 \times 10^1$	$1.96 \times 10^1$	$1.97 \times 10^3$
$f_{T2}/\Lambda^4$	$3.25 \times 10^{-1}$	$1.02 \times 10^1$	2.39	$2.36 \times 10^2$
$f_{T5}/\Lambda^4$	$1.01 \times 10^1$	$3.88 \times 10^2$	$5.79 \times 10^1$	$6.31 \times 10^3$
$f_{T6}/\Lambda^4$	$2.79 \times 10^1$	$8.71 \times 10^2$	$2.12 \times 10^2$	$2.10 \times 10^4$
$f_{T7}/\Lambda^4$	3.45	$1.10 \times 10^2$	26.13	$2.51 \times 10^3$

### Acknowledgments

A. G. R. and M. A. H. R. thank SNI and PROFEXCE (México). The numerical calculations reported in this paper were partially performed at TUBITAK ULAKBIM, High Performance and Grid Computing Center (TRUBA resources).

TABLE II: Summary of the total cross-sections of the process  $ep \rightarrow e^- \gamma^* p \rightarrow eW\gamma q'X$  for  $\sqrt{s} = 1.30, 1.98$  TeV at the LHeC and  $\sqrt{s} = 1.30, 1.98$  TeV at the FCC-he depending on thirteen anomalous couplings obtained by dimension-8 operators. The total cross-sections for each coupling are calculated with the values of  $1 \times 10^{-8} \text{ GeV}^{-4}$  and  $5 \times 10^{-9} \text{ GeV}^{-4}$  at the LHeC and the FCC-he, respectively.

$\sigma(ep \rightarrow e^- \gamma^* p \rightarrow eW\gamma q'X)$ (pb)				
	LHeC		FCC-he	
	Hadronic channel		Hadronic channel	
SM	$1.54 \times 10^{-2}$	$4.51 \times 10^{-2}$	$4.94 \times 10^{-2}$	$1.34 \times 10^{-1}$
Couplings	$\sqrt{s} = 1.30$ TeV	$\sqrt{s} = 1.98$ TeV	$\sqrt{s} = 3.46$ TeV	$\sqrt{s} = 5.29$ TeV
$f_{M0}/\Lambda^4$	$5.79 \times 10^{-2}$	$9.38 \times 10^{-1}$	$1.79 \times 10^{-1}$	2.50
$f_{M1}/\Lambda^4$	$6.05 \times 10^{-2}$	$6.89 \times 10^{-1}$	$7.34 \times 10^{-1}$	5.88
$f_{M2}/\Lambda^4$	1.84	$3.84 \times 10^1$	5.70	$1.02 \times 10^2$
$f_{M3}/\Lambda^4$	2.08	$2.82 \times 10^1$	$2.98 \times 10^1$	$2.49 \times 10^2$
$f_{M4}/\Lambda^4$	$1.54 \times 10^{-1}$	2.98	$4.79 \times 10^{-1}$	7.88
$f_{M5}/\Lambda^4$	$1.80 \times 10^{-1}$	2.22	2.32	$1.92 \times 10^1$
$f_{M7}/\Lambda^4$	$2.92 \times 10^{-2}$	$2.15 \times 10^{-1}$	$2.26 \times 10^{-1}$	1.59
$f_{T0}/\Lambda^4$	2.27	$7.24 \times 10^1$	$1.51 \times 10^1$	$5.07 \times 10^2$
$f_{T1}/\Lambda^4$	$1.14 \times 10^1$	$2.15 \times 10^2$	$5.81 \times 10^2$	$7.07 \times 10^3$
$f_{T2}/\Lambda^4$	1.21	$2.50 \times 10^1$	$5.11 \times 10^1$	$6.54 \times 10^2$
$f_{T5}/\Lambda^4$	$2.42 \times 10^1$	$7.76 \times 10^2$	$1.62 \times 10^2$	$5.45 \times 10^3$
$f_{T6}/\Lambda^4$	$1.22 \times 10^2$	$2.31 \times 10^3$	$6.28 \times 10^3$	$7.65 \times 10^4$
$f_{T7}/\Lambda^4$	$1.30 \times 10^1$	$2.68 \times 10^2$	$5.50 \times 10^2$	$7.02 \times 10^3$

- 
- [1] S. L. Glashow, *Nucl. Phys.* **22**, 579 (1961).  
[2] A. Salam, J. C., *Phys. Lett.* **13**, 168 (1964).  
[3] S. Weinberg, *Phys. Rev. Lett.* **19**, 1264 (1967).  
[4] P. Azzi, *etal.*, Report from Working Group 1 on the Physics of the HL-LHC, and Perspectives

TABLE III: Effects of selected cuts on the cross-sections of the process  $\sigma(ep \rightarrow e^- \gamma^* p \rightarrow eW\gamma q' X)$  for SM and BSM for various anomalous couplings at 1.98 TeV and 5.29 TeV. The cross-sections are calculated with the values of  $5 \times 10^{-10} \text{ GeV}^{-4}$  and  $5 \times 10^{-11} \text{ GeV}^{-4}$  at the LHeC and the FCC-he, respectively. The hadronic decay of  $W$ -boson is considered.

$\sigma(ep \rightarrow e^- \gamma^* p \rightarrow eW\gamma q' X)$ (pb)								
	LHeC				FCC-he			
	$\sqrt{s} = 1.98 \text{ TeV}$				$\sqrt{s} = 5.29 \text{ TeV}$			
Couplings	No Cuts	Cuts-0	Cuts-1	Cuts-2	No Cuts	Cuts-0	Cuts-1	Cuts-2
$SM$	6.18	0.11	0.08	0.046	15.91	0.58	0.23	0.13
$f_{M0}/\Lambda^4$	6.42	0.12	0.08	0.05	18.16	0.57	0.25	0.14
$f_{M2}/\Lambda^4$	7.10	0.29	0.19	0.14	19.51	1.37	0.25	0.14
$f_{M5}/\Lambda^4$	7.65	0.12	0.09	0.05	16.53	0.59	0.23	0.13
$f_{T0}/\Lambda^4$	6.91	0.53	0.30	0.22	16.68	3.65	0.44	0.17
$f_{T6}/\Lambda^4$	12.31	8.25	7.69	5.72	80.92	65.2	33.71	7.47
$f_{T7}/\Lambda^4$	6.22	1.19	0.94	0.69	21.42	8.80	3.31	0.81

at the HE-LHC, arXiv:1902.04070 [hep-ph].

- [5] J. L. A. Fernandez, *et al.*, [LHeC Study Group], J. Phys. G39, 075001 (2012).
- [6] J. L. A. Fernandez, *et al.*, [LHeC Study Group], arXiv:1211.5102.
- [7] J. L. A. Fernandez, *et al.*, arXiv:1211.4831.
- [8] O. Brüning and M. Klein, *Mod. Phys. Lett. A28*, 1330011 (2013).
- [9] Oliver Brüning, John Jowett, Max Klein, Dario Pellegrini, Daniel Schulte and Frank Zimmermann, EDMS 17979910 FCC-ACC-RPT-0012, V1.0, 6 April, 2017. <https://fcc.web.cern.ch/Documents/FCCheBaselineParameters.pdf>.
- [10] J. Brau, *et al.*, The International Linear Collider (ILC): A global project, [https://ilchome.web.cern.ch/sites/ilchome.web.cern.ch/files/ILC\\_European\\_Strategy\\_Document-ILCGeneral.pdf](https://ilchome.web.cern.ch/sites/ilchome.web.cern.ch/files/ILC_European_Strategy_Document-ILCGeneral.pdf) (2018).
- [11] P. N. Burrows, *et al.*, The Compact Linear Collider (CLIC)-2018 Summary Report, **CERN Yellow Rep.Monogr. 1802 (2018) 1-98**, arXiv:1812.06018 [physics.acc-ph].
- [12] M. Ahmad, *et al.*, (The CEPC-SPPC Study Group), CEPC conceptual design report: Volume

TABLE IV: Sensitivity measures on aQGC at the 95% C. L. via  $ep \rightarrow e^- \gamma^* p \rightarrow eW\gamma q'X$  for  $\sqrt{s} = 1.30, 1.98$  TeV at the LHeC.

$\sqrt{s} = 1.30$ TeV, Leptonic channel				
Couplings (TeV <sup>-4</sup> )	10 fb <sup>-1</sup>	30 fb <sup>-1</sup>	50 fb <sup>-1</sup>	100 fb <sup>-1</sup>
$f_{M0}/\Lambda^4$	$[-3.27;3.28] \times 10^3$	$[-2.48;2.49] \times 10^3$	$[-2.18;2.19] \times 10^3$	$[-1.84;1.85] \times 10^3$
$f_{M1}/\Lambda^4$	$[-3.51;4.57] \times 10^3$	$[-2.56;3.62] \times 10^3$	$[-2.20;3.26] \times 10^3$	$[-1.78;2.85] \times 10^3$
$f_{M2}/\Lambda^4$	$[-5.02;5.01] \times 10^2$	$[-3.81;3.80] \times 10^2$	$[-3.36;3.35] \times 10^2$	$[-2.82;2.81] \times 10^2$
$f_{M3}/\Lambda^4$	$[-5.39;6.99] \times 10^2$	$[-3.93;5.54] \times 10^2$	$[-3.38;4.99] \times 10^2$	$[-2.74;4.35] \times 10^2$
$f_{M4}/\Lambda^4$	$[-1.81;1.82] \times 10^3$	$[-1.37;1.38] \times 10^3$	$[-1.21;1.22] \times 10^3$	$[-1.01;1.02] \times 10^3$
$f_{M5}/\Lambda^4$	$[-2.56;1.92] \times 10^3$	$[-2.03;1.39] \times 10^3$	$[-1.84;1.19] \times 10^3$	$[-1.61;0.97] \times 10^3$
$f_{M7}/\Lambda^4$	$[-0.91;0.70] \times 10^4$	$[-0.72;0.51] \times 10^4$	$[-0.65;0.44] \times 10^4$	$[-0.57;0.35] \times 10^4$
$f_{T0}/\Lambda^4$	$[-4.18;4.26] \times 10^2$	$[-3.17;3.24] \times 10^2$	$[-2.78;2.86] \times 10^2$	$[-2.33;2.41] \times 10^2$
$f_{T1}/\Lambda^4$	$[-2.43;2.66] \times 10^2$	$[-1.82;2.05] \times 10^2$	$[-1.59;1.82] \times 10^2$	$[-1.32;1.55] \times 10^2$
$f_{T2}/\Lambda^4$	$[-0.66;0.79] \times 10^3$	$[-0.49;0.62] \times 10^3$	$[-0.42;0.55] \times 10^3$	$[-0.35;0.48] \times 10^3$
$f_{T5}/\Lambda^4$	$[-1.27;1.30] \times 10^2$	$[-9.64;9.88] \times 10^1$	$[-8.47;8.71] \times 10^1$	$[-7.10;7.35] \times 10^1$
$f_{T6}/\Lambda^4$	$[-7.57;7.94] \times 10^1$	$[-5.71;6.08] \times 10^1$	$[-5.00;5.37] \times 10^1$	$[-4.18;4.55] \times 10^1$
$f_{T7}/\Lambda^4$	$[-2.08;2.34] \times 10^2$	$[-1.55;1.81] \times 10^2$	$[-1.35;1.61] \times 10^2$	$[-1.12;1.38] \times 10^2$
$\sqrt{s} = 1.98$ TeV				
$f_{M0}/\Lambda^4$	$[-8.86;8.89] \times 10^2$	$[-6.73;6.76] \times 10^2$	$[-5.92;5.95] \times 10^2$	$[-4.97;5.00] \times 10^2$
$f_{M1}/\Lambda^4$	$[-1.07;1.28] \times 10^3$	$[-0.79;1.00] \times 10^3$	$[-0.68;0.90] \times 10^3$	$[-0.56;0.78] \times 10^3$
$f_{M2}/\Lambda^4$	$[-1.35;1.34] \times 10^2$	$[-1.03;1.02] \times 10^2$	$[-9.00;8.99] \times 10^1$	$[-7.57;7.56] \times 10^1$
$f_{M3}/\Lambda^4$	$[-1.66;1.92] \times 10^2$	$[-1.24;1.49] \times 10^2$	$[-1.07;1.33] \times 10^2$	$[-0.88;1.14] \times 10^2$
$f_{M4}/\Lambda^4$	$[-4.86;4.88] \times 10^2$	$[-3.69;3.70] \times 10^2$	$[-3.25;3.26] \times 10^2$	$[-2.73;2.75] \times 10^2$
$f_{M5}/\Lambda^4$	$[-0.71;0.59] \times 10^3$	$[-0.55;0.44] \times 10^3$	$[-0.50;0.38] \times 10^3$	$[-0.43;0.31] \times 10^3$
$f_{M7}/\Lambda^4$	$[-2.57;2.14] \times 10^3$	$[-2.01;1.58] \times 10^3$	$[-1.80;1.37] \times 10^3$	$[-1.55;1.12] \times 10^3$
$f_{T0}/\Lambda^4$	$[-9.00;9.03] \times 10^1$	$[-6.83;6.86] \times 10^1$	$[-6.01;6.04] \times 10^1$	$[-5.05;5.08] \times 10^1$
$f_{T1}/\Lambda^4$	$[-5.91;6.09] \times 10^1$	$[-4.47;4.65] \times 10^1$	$[-3.92;4.10] \times 10^1$	$[-3.28;3.47] \times 10^1$
$f_{T2}/\Lambda^4$	$[-1.60;1.78] \times 10^2$	$[-1.20;1.38] \times 10^2$	$[-1.04;1.23] \times 10^2$	$[-0.86;1.05] \times 10^2$
$f_{T5}/\Lambda^4$	$[-2.69;2.80] \times 10^1$	$[-2.03;2.14] \times 10^1$	$[-1.78;1.89] \times 10^1$	$[-1.49;1.60] \times 10^1$
$f_{T6}/\Lambda^4$	$[-1.77;1.89] \times 10^1$	$[-1.33;1.45] \times 10^1$	$[-1.17;1.28] \times 10^1$	$[-0.97;1.09] \times 10^1$
$f_{T7}/\Lambda^4$	$[-5.05;5.29] \times 10^1$	$[-3.81;4.05] \times 10^1$	$[-3.34;3.58] \times 10^1$	$[-2.79;3.03] \times 10^1$



TABLE V: Sensitivity measures on aQGC at the 95% C. L. via  $ep \rightarrow e^- \gamma^* p \rightarrow eW\gamma q'X$  for  $\sqrt{s} = 3.46, 5.29$  TeV at the FCC-he.

$\sqrt{s} = 3.46$ TeV, Leptonic channel				
Couplings (TeV <sup>-4</sup> )	100 fb <sup>-1</sup>	300 fb <sup>-1</sup>	500 fb <sup>-1</sup>	1000 fb <sup>-1</sup>
$f_{M0}/\Lambda^4$	$[-6.70;6.81] \times 10^2$	$[-5.08;5.19] \times 10^2$	$[-4.47;4.57] \times 10^2$	$[-3.75;3.85] \times 10^2$
$f_{M1}/\Lambda^4$	$[-0.62;0.88] \times 10^3$	$[-0.44;0.71] \times 10^3$	$[-0.38;0.64] \times 10^3$	$[-0.30;0.57] \times 10^3$
$f_{M2}/\Lambda^4$	$[-1.03;1.00] \times 10^2$	$[-7.87;7.63] \times 10^1$	$[-6.95;6.71] \times 10^1$	$[-5.86;5.62] \times 10^1$
$f_{M3}/\Lambda^4$	$[-1.11;1.13] \times 10^2$	$[-8.42;8.65] \times 10^1$	$[-7.40;7.63] \times 10^1$	$[-6.21;6.43] \times 10^1$
$f_{M4}/\Lambda^4$	$[-3.75;3.77] \times 10^2$	$[-2.85;2.87] \times 10^2$	$[-2.51;2.52] \times 10^2$	$[-2.11;2.12] \times 10^2$
$f_{M5}/\Lambda^4$	$[-4.17;4.08] \times 10^2$	$[-3.18;3.09] \times 10^2$	$[-2.80;2.71] \times 10^2$	$[-2.36;2.27] \times 10^2$
$f_{M7}/\Lambda^4$	$[-1.78;1.39] \times 10^3$	$[-1.40;1.01] \times 10^3$	$[-1.26;0.88] \times 10^3$	$[-1.10;0.71] \times 10^3$
$f_{T0}/\Lambda^4$	$[-6.71;6.93] \times 10^1$	$[-5.08;5.30] \times 10^1$	$[-4.45;4.67] \times 10^1$	$[-3.73;3.95] \times 10^1$
$f_{T1}/\Lambda^4$	$[-3.49;3.52] \times 10^1$	$[-2.64;2.68] \times 10^1$	$[-2.33;2.36] \times 10^1$	$[-1.95;1.98] \times 10^1$
$f_{T2}/\Lambda^4$	$[-0.89;1.14] \times 10^2$	$[-0.65;0.90] \times 10^2$	$[-0.56;0.81] \times 10^2$	$[-0.45;0.71] \times 10^2$
$f_{T5}/\Lambda^4$	$[-2.02;2.03] \times 10^1$	$[-1.53;1.55] \times 10^1$	$[-1.35;1.36] \times 10^1$	$[-1.13;1.15] \times 10^1$
$f_{T6}/\Lambda^4$	$[-0.94;1.19] \times 10^1$	$[-0.69;0.94] \times 10^1$	$[-0.60;0.84] \times 10^1$	$[-0.48;0.73] \times 10^1$
$f_{T7}/\Lambda^4$	$[-0.28;0.33] \times 10^2$	$[-0.20;0.26] \times 10^2$	$[-0.18;0.23] \times 10^2$	$[-0.15;0.20] \times 10^2$
$\sqrt{s} = 5.29$ TeV				
$f_{M0}/\Lambda^4$	$[-1.19;1.24] \times 10^2$	$[-9.00;9.45] \times 10^1$	$[-7.90;8.34] \times 10^1$	$[-6.61;7.05] \times 10^1$
$f_{M1}/\Lambda^4$	$[-1.28;1.53] \times 10^2$	$[-0.95;1.20] \times 10^2$	$[-0.82;1.07] \times 10^2$	$[-0.67;0.92] \times 10^2$
$f_{M2}/\Lambda^4$	$[-1.84;1.82] \times 10^1$	$[-1.40;1.38] \times 10^1$	$[-1.23;1.22] \times 10^1$	$[-1.04;1.02] \times 10^1$
$f_{M3}/\Lambda^4$	$[-2.06;2.22] \times 10^1$	$[-1.54;1.70] \times 10^1$	$[-1.35;1.51] \times 10^1$	$[-1.12;1.28] \times 10^1$
$f_{M4}/\Lambda^4$	$[-6.62;6.68] \times 10^1$	$[-5.02;5.09] \times 10^1$	$[-4.42;4.48] \times 10^1$	$[-3.71;3.77] \times 10^1$
$f_{M5}/\Lambda^4$	$[-0.83;0.72] \times 10^2$	$[-0.65;0.54] \times 10^2$	$[-0.58;0.47] \times 10^2$	$[-0.49;0.39] \times 10^2$
$f_{M7}/\Lambda^4$	$[-2.98;2.76] \times 10^2$	$[-2.29;2.07] \times 10^2$	$[-2.03;1.81] \times 10^2$	$[-1.73;1.50] \times 10^2$
$f_{T0}/\Lambda^4$	$[-8.18;8.23]$	$[-6.21;6.26]$	$[-5.46;5.51]$	$[-4.59;4.64]$
$f_{T1}/\Lambda^4$	$[-4.37;4.60]$	$[-3.29;3.52]$	$[-2.88;3.11]$	$[-2.41;2.64]$
$f_{T2}/\Lambda^4$	$[-1.23;1.36] \times 10^1$	$[-0.92;1.05] \times 10^1$	$[-0.81;0.93] \times 10^1$	$[-0.67;0.79] \times 10^1$
$f_{T5}/\Lambda^4$	$[-2.41;2.60]$	$[-1.81;1.99]$	$[-1.58;1.77]$	$[-1.31;1.50]$
$f_{T6}/\Lambda^4$	$[-1.22;1.53]$	$[-0.89;1.21]$	$[-0.77;1.08]$	$[-0.63;0.94]$
$f_{T7}/\Lambda^4$	$[-3.83;4.07]$	$[-2.88;3.13]$	$[-2.52;2.77]$	$[-2.10;2.35]$

TABLE VI: Sensitivity measures on aQGC at the 95% C. L. via  $ep \rightarrow e^- \gamma^* p \rightarrow eW\gamma q'X$  for  $\sqrt{s} = 1.30, 1.98$  TeV at the LHeC.

$\sqrt{s} = 1.30$ TeV, Hadronic channel				
Couplings ( $\text{TeV}^{-4}$ )	$10 \text{ fb}^{-1}$	$30 \text{ fb}^{-1}$	$50 \text{ fb}^{-1}$	$100 \text{ fb}^{-1}$
$f_{M0}/\Lambda^4$	$[-2.37;2.41] \times 10^3$	$[-1.80;1.84] \times 10^3$	$[-1.59;1.62] \times 10^3$	$[-1.32;1.36] \times 10^3$
$f_{M1}/\Lambda^4$	$[-1.95;2.59] \times 10^3$	$[-1.41;2.06] \times 10^3$	$[-1.21;1.86] \times 10^3$	$[-0.98;1.62] \times 10^3$
$f_{M2}/\Lambda^4$	$[-3.68;3.61] \times 10^2$	$[-2.81;2.73] \times 10^2$	$[-2.47;2.40] \times 10^2$	$[-2.09;2.01] \times 10^2$
$f_{M3}/\Lambda^4$	$[-2.93;3.98] \times 10^2$	$[-2.12;3.17] \times 10^2$	$[-1.82;2.87] \times 10^2$	$[-1.47;2.51] \times 10^2$
$f_{M4}/\Lambda^4$	$[-1.31;1.33] \times 10^3$	$[-9.92;10.13] \times 10^2$	$[-8.72;8.93] \times 10^2$	$[-7.31;7.53] \times 10^2$
$f_{M5}/\Lambda^4$	$[-1.44;1.07] \times 10^3$	$[-1.15;0.77] \times 10^3$	$[-1.04;0.66] \times 10^3$	$[-0.91;0.54] \times 10^3$
$f_{M7}/\Lambda^4$	$[-5.18;3.85] \times 10^3$	$[-4.12;2.79] \times 10^3$	$[-3.73;2.39] \times 10^3$	$[-3.26;1.93] \times 10^3$
$f_{T0}/\Lambda^4$	$[-3.28;3.29] \times 10^2$	$[-2.49;2.50] \times 10^2$	$[-2.19;2.20] \times 10^2$	$[-1.84;1.85] \times 10^2$
$f_{T1}/\Lambda^4$	$[-1.31;1.63] \times 10^2$	$[-0.96;1.28] \times 10^2$	$[-0.83;1.15] \times 10^2$	$[-0.68;1.00] \times 10^2$
$f_{T2}/\Lambda^4$	$[-4.06;4.98] \times 10^2$	$[-2.98;3.91] \times 10^2$	$[-2.58;3.50] \times 10^2$	$[-2.11;3.03] \times 10^2$
$f_{T5}/\Lambda^4$	$[-9.54;10.51] \times 10^1$	$[-7.14;8.11] \times 10^1$	$[-6.23;7.20] \times 10^1$	$[-5.17;6.13] \times 10^1$
$f_{T6}/\Lambda^4$	$[-3.85;5.15] \times 10^1$	$[-2.79;4.09] \times 10^1$	$[-2.40;3.70] \times 10^1$	$[-1.94;3.24] \times 10^1$
$f_{T7}/\Lambda^4$	$[-1.23;1.52] \times 10^2$	$[-0.90;1.20] \times 10^2$	$[-0.78;1.08] \times 10^2$	$[-0.64;0.93] \times 10^2$
$\sqrt{s} = 1.98$ TeV				
$f_{M0}/\Lambda^4$	$[-6.76;6.89] \times 10^2$	$[-5.13;5.25] \times 10^2$	$[-4.50;4.63] \times 10^2$	$[-3.78;3.90] \times 10^2$
$f_{M1}/\Lambda^4$	$[-7.10;8.91] \times 10^2$	$[-5.21;7.02] \times 10^2$	$[-4.49;6.30] \times 10^2$	$[-3.66;5.47] \times 10^2$
$f_{M2}/\Lambda^4$	$[-1.05;1.04] \times 10^2$	$[-7.96;7.86] \times 10^1$	$[-7.02;6.91] \times 10^1$	$[-5.91;5.80] \times 10^1$
$f_{M3}/\Lambda^4$	$[-1.07;1.38] \times 10^2$	$[-0.78;1.09] \times 10^2$	$[-0.67;0.98] \times 10^2$	$[-0.54;0.86] \times 10^2$
$f_{M4}/\Lambda^4$	$[-3.76;3.79] \times 10^2$	$[-2.85;2.89] \times 10^2$	$[-2.51;2.54] \times 10^2$	$[-2.10;2.14] \times 10^2$
$f_{M5}/\Lambda^4$	$[-4.90;3.93] \times 10^2$	$[-3.86;2.89] \times 10^2$	$[-3.46;2.49] \times 10^2$	$[-3.00;2.03] \times 10^2$
$f_{M7}/\Lambda^4$	$[-1.79;1.42] \times 10^3$	$[-1.41;1.04] \times 10^3$	$[-1.27;0.90] \times 10^3$	$[-1.10;0.73] \times 10^3$
$f_{T0}/\Lambda^4$	$[-7.54;7.62] \times 10^1$	$[-5.72;5.80] \times 10^1$	$[-5.03;5.11] \times 10^1$	$[-4.23;4.30] \times 10^1$
$f_{T1}/\Lambda^4$	$[-3.99;4.85] \times 10^1$	$[-2.94;3.80] \times 10^1$	$[-2.54;3.40] \times 10^1$	$[-2.08;2.94] \times 10^1$
$f_{T2}/\Lambda^4$	$[-1.17;1.43] \times 10^2$	$[-0.86;1.12] \times 10^2$	$[-0.74;1.01] \times 10^2$	$[-0.61;0.87] \times 10^2$
$f_{T5}/\Lambda^4$	$[-2.31;2.32] \times 10^1$	$[-1.75;1.76] \times 10^1$	$[-1.54;1.55] \times 10^1$	$[-1.29;1.31] \times 10^1$
$f_{T6}/\Lambda^4$	$[-1.30;1.39] \times 10^1$	$[-0.98;1.07] \times 10^1$	$[-0.86;0.94] \times 10^1$	$[-0.71;0.80] \times 10^1$
$f_{T7}/\Lambda^4$	$[-3.50;4.42] \times 10^1$	$[-2.57;3.49] \times 10^1$	$[-2.21;3.13] \times 10^1$	$[-1.80;2.72] \times 10^1$

TABLE VII: Sensitivity measures on aQGC at the 95% C. L. via  $ep \rightarrow e^- \gamma^* p \rightarrow eW\gamma q'X$  for  $\sqrt{s} = 3.46, 5.29$  TeV at the FCC-he.

$\sqrt{s} = 3.46$ TeV, Hadronic channel				
Couplings (TeV <sup>-4</sup> )	100 fb <sup>-1</sup>	300 fb <sup>-1</sup>	500 fb <sup>-1</sup>	1000 fb <sup>-1</sup>
$f_{M0}/\Lambda^4$	$[-5.12;5.13] \times 10^2$	$[-3.89;3.90] \times 10^2$	$[-3.42;3.44] \times 10^2$	$[-2.88;2.89] \times 10^2$
$f_{M1}/\Lambda^4$	$[-1.93;2.58] \times 10^2$	$[-1.40;2.05] \times 10^2$	$[-1.20;1.85] \times 10^2$	$[-0.97;1.62] \times 10^2$
$f_{M2}/\Lambda^4$	$[-0.87;0.70] \times 10^2$	$[-0.68;0.52] \times 10^2$	$[-0.61;0.45] \times 10^2$	$[-0.53;0.37] \times 10^2$
$f_{M3}/\Lambda^4$	$[-2.94;3.93] \times 10^1$	$[-2.13;3.12] \times 10^1$	$[-1.83;2.82] \times 10^1$	$[-1.48;2.47] \times 10^1$
$f_{M4}/\Lambda^4$	$[-2.78;2.89] \times 10^2$	$[-2.10;2.21] \times 10^2$	$[-1.84;1.95] \times 10^2$	$[-1.54;1.65] \times 10^2$
$f_{M5}/\Lambda^4$	$[-1.53;1.02] \times 10^2$	$[-1.24;0.73] \times 10^2$	$[-1.13;0.62] \times 10^2$	$[-1.00;0.49] \times 10^2$
$f_{M7}/\Lambda^4$	$[-5.29;3.76] \times 10^2$	$[-4.24;2.71] \times 10^2$	$[-3.85;2.32] \times 10^2$	$[-3.39;1.86] \times 10^2$
$f_{T0}/\Lambda^4$	$[-4.62;5.00] \times 10^1$	$[-3.47;3.85] \times 10^1$	$[-3.03;3.41] \times 10^1$	$[-2.52;2.90] \times 10^1$
$f_{T1}/\Lambda^4$	$[-0.74;0.81] \times 10^1$	$[-0.56;0.62] \times 10^1$	$[-0.49;0.55] \times 10^1$	$[-0.40;0.47] \times 10^1$
$f_{T2}/\Lambda^4$	$[-2.26;2.99] \times 10^1$	$[-1.64;2.37] \times 10^1$	$[-1.41;2.14] \times 10^1$	$[-1.14;1.87] \times 10^1$
$f_{T5}/\Lambda^4$	$[-1.42;1.51] \times 10^1$	$[-1.07;1.16] \times 10^1$	$[-0.94;1.02] \times 10^1$	$[-0.78;0.87] \times 10^1$
$f_{T6}/\Lambda^4$	$[-2.12;2.62]$	$[-1.56;2.05]$	$[-1.34;1.84]$	$[-1.10;1.60]$
$f_{T7}/\Lambda^4$	$[-7.18;8.88]$	$[-5.27;6.98]$	$[-4.55;6.26]$	$[-3.72;5.42]$
$\sqrt{s} = 5.29$ TeV				
$f_{M0}/\Lambda^4$	$[-1.53;1.58] \times 10^2$	$[-1.15;1.21] \times 10^2$	$[-1.01;1.07] \times 10^2$	$[-0.85;0.90] \times 10^1$
$f_{M1}/\Lambda^4$	$[-0.90;1.12] \times 10^2$	$[-0.66;0.88] \times 10^2$	$[-0.57;0.79] \times 10^2$	$[-0.46;0.68] \times 10^2$
$f_{M2}/\Lambda^4$	$[-2.41;2.33] \times 10^1$	$[-1.84;1.77] \times 10^1$	$[-1.62;1.55] \times 10^1$	$[-1.37;1.30] \times 10^1$
$f_{M3}/\Lambda^4$	$[-1.30;1.84] \times 10^1$	$[-0.94;1.47] \times 10^1$	$[-0.80;1.34] \times 10^1$	$[-0.64;1.18] \times 10^1$
$f_{M4}/\Lambda^4$	$[-8.44;8.67] \times 10^1$	$[-6.39;6.62] \times 10^1$	$[-5.61;5.84] \times 10^1$	$[-4.70;4.93] \times 10^1$
$f_{M5}/\Lambda^4$	$[-6.23;4.81] \times 10^1$	$[-4.93;3.51] \times 10^1$	$[-4.44;3.02] \times 10^1$	$[-3.87;2.45] \times 10^1$
$f_{M7}/\Lambda^4$	$[-2.19;1.83] \times 10^2$	$[-1.71;1.35] \times 10^2$	$[-1.53;1.17] \times 10^2$	$[-1.32;0.96] \times 10^2$
$f_{T0}/\Lambda^4$	$[-1.04;1.10] \times 10^1$	$[-0.78;0.84] \times 10^1$	$[-0.68;0.74] \times 10^1$	$[-0.57;0.63] \times 10^1$
$f_{T1}/\Lambda^4$	$[-2.53;3.21]$	$[-1.85;2.53]$	$[-1.60;2.27]$	$[-1.30;1.97]$
$f_{T2}/\Lambda^4$	$[-0.82;1.10] \times 10^1$	$[-0.59;0.88] \times 10^1$	$[-0.51;0.79] \times 10^1$	$[-0.41;0.69] \times 10^1$
$f_{T5}/\Lambda^4$	$[-3.17;3.30]$	$[-2.39;2.52]$	$[-2.10;2.23]$	$[-1.75;1.89]$
$f_{T6}/\Lambda^4$	$[-8.17;9.32] \times 10^{-1}$	$[-6.08;7.23] \times 10^{-1}$	$[-5.29;6.44] \times 10^{-1}$	$[-4.37;5.51] \times 10^{-1}$
$f_{T7}/\Lambda^4$	$[-2.35;3.48]$	$[-1.68;2.81]$	$[-1.43;2.56]$	$[-1.14;2.27]$

TABLE VIII:  $Q_{max}$  dependence of the sensitivity measures on aQGC at the 95% C. L. via  $ep \rightarrow e^- \gamma^* p \rightarrow eW\gamma q'X$  for  $\mathcal{L} = 1000 \text{ fb}^{-1}$  and  $\sqrt{s} = 5.29 \text{ TeV}$  at the FCC-he. The hadronic decay of  $W$ -boson is considered.

Couplings ( $\text{TeV}^{-4}$ )	$Q_{max} = 1.41 \text{ GeV}$	$Q_{max} = 8 \text{ GeV}$
$f_{M0}/\Lambda^4$	$[-1.09;0.91] \times 10^2$	$[-9.43;9.36] \times 10^1$
$f_{M1}/\Lambda^4$	$[-6.68;6.10] \times 10^1$	$[-6.81;5.24] \times 10^1$
$f_{M2}/\Lambda^4$	$[-1.77;1.29] \times 10^1$	$[-1.59;1.28] \times 10^1$
$f_{M3}/\Lambda^4$	$[-1.17;0.84] \times 10^1$	$[-1.11;0.79] \times 10^1$
$f_{M4}/\Lambda^4$	$[-5.11;6.12] \times 10^1$	$[-5.16;5.28] \times 10^1$
$f_{M5}/\Lambda^4$	$[-3.74;3.24] \times 10^1$	$[-3.84;2.90] \times 10^1$
$f_{M7}/\Lambda^4$	$[-1.14;1.40] \times 10^2$	$[-1.18;1.22] \times 10^2$
$f_{T0}/\Lambda^4$	$[-6.76;6.94]$	$[-6.12;6.82]$
$f_{T1}/\Lambda^4$	$[-2.09;1.60]$	$[-1.89;1.58]$
$f_{T2}/\Lambda^4$	$[-6.05;5.98]$	$[-6.11;5.28]$
$f_{T5}/\Lambda^4$	$[-3.69;3.72]$	$[-3.41;3.59]$
$f_{T6}/\Lambda^4$	$[-5.07;6.14] \times 10^{-1}$	$[-4.94;5.60] \times 10^{-1}$
$f_{T7}/\Lambda^4$	$[-1.75;1.92]$	$[-1.54;1.93]$

2-Physics & Detector, arXiv:1811.10545 [hep-ex].

- [13] M. Bicer, *et al.*, [TLEP design study working group collaboration]. First look at the physics case of TLEP. *JHEP* **01**, 164 (2014)
- [14] R. Barate, *et al.*, [ALEPH Collaboration], *Phys. Lett.* **B462**, 389 (1999).
- [15] P. Abreu, *et al.*, [DELPHI Collaboration], *Phys. Lett.* **B459**, 382 (1999).
- [16] M. Acciarri, *et al.*, [L3 Collaboration], *Phys. Lett.* **B467**, 171 (1999).
- [17] G. Abbiendi, *et al.*, [OPAL Collaboration], *Eur. Phys. J.* **C8**, 191 (1999).
- [18] K. Gounder, [CDF Collaboration], hep-ex/9903038.
- [19] B. Abbott, *et al.*, [D Collaboration], *Phys. Rev.* **D62**, 052005 (2000).
- [20] S. Chatrchyan, *etal.*, [CMS Collaboration], *JHEP* **07**, 116 (2013).
- [21] M. Aaboud, *et al.*, [ATLAS Collaboration], *Eur. Phys. J.* **C77**, 646 (2017).
- [22] V. Ari, E. Gurkanli, A. A. Billur and M. Köksal, arXiv:1812.07187 [hep-ph].

- [23] V. Ari, E. Gurkanli, A. Gutiérrez-Rodríguez, M. A. Hernández-Ruíz, and M. Köksal, *Eur. Phys. J. Plus* **135**, 336 (2020), arXiv:1911.03993 [hep-ph].
- [24] W. J. Stirling and A. Werthenbach, *Eur. Phys. J.* **C14**, 103 (2000).
- [25] G. A. Leil and W. J. Stirling, *J. Phys.* **G21**, 517 (1995).
- [26] P.J. Dervan, A. Signer, W.J. Stirling, and A. Werthenbach, *J. Phys.* **G26**, 607 (2000).
- [27] C. Chong, *et al.*, *Eur. Phys. J.* **C74**, 3166 (2014).
- [28] M. Köksal and A. Senol, *Int. J. Mod. Phys.* **A30**, 1550107 (2015).
- [29] C. Chen, *et al.*, *Eur. Phys. J.* **C74**, 3166 (2014).
- [30] W. J. Stirling and A. Werthenbach, *Phys. Lett.* **B466**, 369 (1999).
- [31] S. Atag and I. Sahin, *Phys. Rev.* **D75**, 073003 (2007).
- [32] O. J. P. Eboli, M. B. Magro, P. G. Mercadante, and S. F. Novaes, *Phys. Rev.* **D52**, 15 (1995).
- [33] I. Sahin, *J. Phys.* **G36**, 075007 (2009).
- [34] M. Köksal, V. Ari and A. Senol, *Adv. High Energy Phys.* **2016**, 8672391 (2016).
- [35] E. Chapon, C. Royon and O. Kepka, *Phys. Rev.* **D81**, 074003 (2010).
- [36] M. Köksal, *Mod. Phys. Lett.* **A29**, 1450184 (2014).
- [37] A. Senol and M. Köksal, *JHEP* **1503**, 139 (2015).
- [38] M. Köksal, *Eur. Phys. J. Plus* **130**, 75 (2015).
- [39] D. Yang, Y. Mao, Q. Li, S. Liu, Z. Xu, and K. Ye, *JHEP* **1304**, 108 (2013).
- [40] O. J. P. Eboli, M. C. Gonzalez-Garcia, and S. M. Lietti, S. F. Novaes, *Phys. Rev.* **D63**, 075008 (2001).
- [41] O. J. P. Eboli, M. C. Gonzalez-Garcia, and S. M. Lietti, *Phys. Rev.* **D69**, 095005 (2004).
- [42] P. J. Bell, *Eur. Phys. J.* **C64**, 25 (2009).
- [43] A. I. Ahmadov, arXiv:1806.03460.
- [44] M. Schonherr, *JHEP* **1807**, 076 (2018).
- [45] Y. Wen, *et al.*, *JHEP* **1503**, 025 (2015).
- [46] K. Ye, D. Yang and Q. Li, *Phys. Rev.* **D88**, 015023 (2013).
- [47] G. Perez, M. Sekulla and D. Zeppenfeld, *Eur. Phys. J.* **C78**, 759 (2018).
- [48] I. Sahin and B. Sahin, *Phys. Rev.* **D86**, 115001 (2012).
- [49] A. Senol and M. Köksal, *Phys. Lett.* **B742**, 143-148 (2015).
- [50] C. Baldenegro, *et al.*, *JHEP* **1706**, 142 (2017).
- [51] S. Fichet, *et al.*, *JHEP* **1502**, 165 (2015).

- [52] T. Pierzchala and K. Piotrkowski, *Nucl. Phys. Proc. Suppl.* **257**, 179 (2008).
- [53] A. Gutiérrez-Rodríguez, C. G. Honorato, J. Montaña and M. A. Pérez, *Phys. Rev.* **D89**, 034003 (2014).
- [54] G. Belanger, F. Boudjema, Y. Kurihara, D. Perret-Gallix, and A. Semenov, *Eur. Phys. J.* **C13**, 283 (2000).
- [55] M. Aaboud, *et al.*, [ATLAS Collaboration], *Eur. Phys. J.* **C77**, 646 (2017).
- [56] O. J. P. Eboli, M. C. Gonzalez-Garcia, and S. F. Novaes, *Nucl. Phys.* **B411**, 381 (1994).
- [57] O. J. P. Eboli, M. C. Gonzalez-Garcia and J. K. Mizukoshi, *Phys. Rev.* **D74**, 073005 (2006).
- [58] C. Degrande, *et al.*, arXiv: 1309.7890.
- [59] X. Rouby, *Ph.D. Thesis*, Universite Catholique de Louvain [UCL-Thesis 135-2008,CMS TS-2009/004], 2008.
- [60] T. Aaltonen, *et al.*, [CDF Collaboration], *Phys. Rev. Lett.* **102**, 222002 (2009).
- [61] T. Aaltonen, *et al.*, [CDF Collaboration], *Phys. Rev. Lett.* **102**, 242001 (2009).
- [62] S. Chatrchyan, *et al.*, [CMS Collaboration], *JHEP* **1201**, 052 (2012).
- [63] S. Chatrchyan, *et al.*, [CMS Collaboration], *JHEP* **1211**, 080 (2012).
- [64] Armen Buniatyan, DIS 2012, 1059-1064.
- [65] R. Li, *et al.*, *Phys. Rev. D* **100**, 053008 (2019).
- [66] J. L. Abelleira Fernandez *et al.* [LHeC Study Group], *J. Phys. G* **39**, 075001 (2012), [arXiv:1206.2913 [physics.acc-ph]].
- [67] J. Alwall, M. Herquet, F. Maltoni, O. Mattelaer and T. Stelzer, *JHEP* **06**, 128 (2011).
- [68] A. Alloul, N. D. Christensen, C. Degrande, C. Duhr and B. Fuks, *Comput. Phys. Commun.* **185**, 2250 (2014), [arXiv:1310.1921 [hep-ph]].
- [69] C. Degrande, C. Duhr, B. Fuks, D. Grellscheid, O. Mattelaer and T. Reiter, *Comput. Phys. Commun.* **183**, 1201 (2012), [arXiv:1108.2040 [hep-ph]].
- [70] I. F. Ginzburg, arXiv:1508.06581 [hep-ph].
- [71] I. F. Ginzburg, G. L. Kotkin, S. L. Panfil, V. G. Serbo and V. I. Telnov, *Nucl. Instrum. Meth.* **A219**, 5 (1984).
- [72] S. J. Brodsky, T. Kinoshita and H. Terazawa, *Phys. Rev.* **D4**, 1532 (1971).
- [73] V. M. Budnev, I. F. Ginzburg, G. V. Meledin and V. G. Serbo, *Phys. Rep.* **15**, 181 (1975).
- [74] H. Terazawa, *Rev. Mod. Phys.* **45**, 615 (1973).
- [75] J. M. Yang, *Annals Phys.* **316**, 529 (2005).

- [76] G. Baur, *et al.*, *Phys. Rep.* **364**, 359 (2002).
- [77] K. Piotrkowski, *Phys. Rev.* **D63**, 071502 (2001).
- [78] A. Belyaev, N. D. Christensen and A. Pukhov, *Comput. Phys. Commun.* **184**, 1729 (2013).
- [79] S. Atag and A. A. Billur, *JHEP* **1011**, 060 (2010).
- [80] S. Atag and E. Gürkanli, *JHEP* **06**, 118 (2016).
- [81] M. Köksal, *J. Phys. G: Nucl. Part. Phys.* **46**, 065003 (2019).
- [82] V. Khachatryan, *et al.*, [CMS Collaboration], *JHEP* **08**, 119 (2016).
- [83] V. Khachatryan, *et al.*, [CMS Collaboration], *JHEP* **06**, 106 (2017).

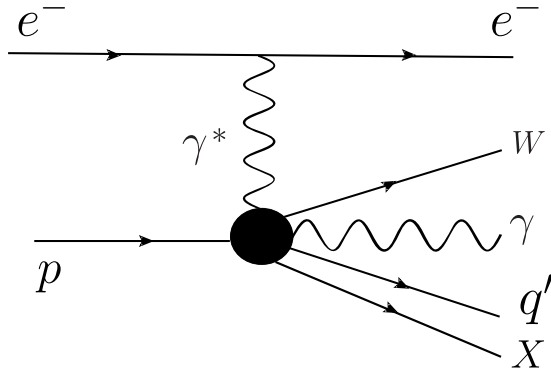


FIG. 1: A schematic diagram for the processes  $e^- p \rightarrow e^- \gamma^* p \rightarrow e^- W \gamma q' X$ .

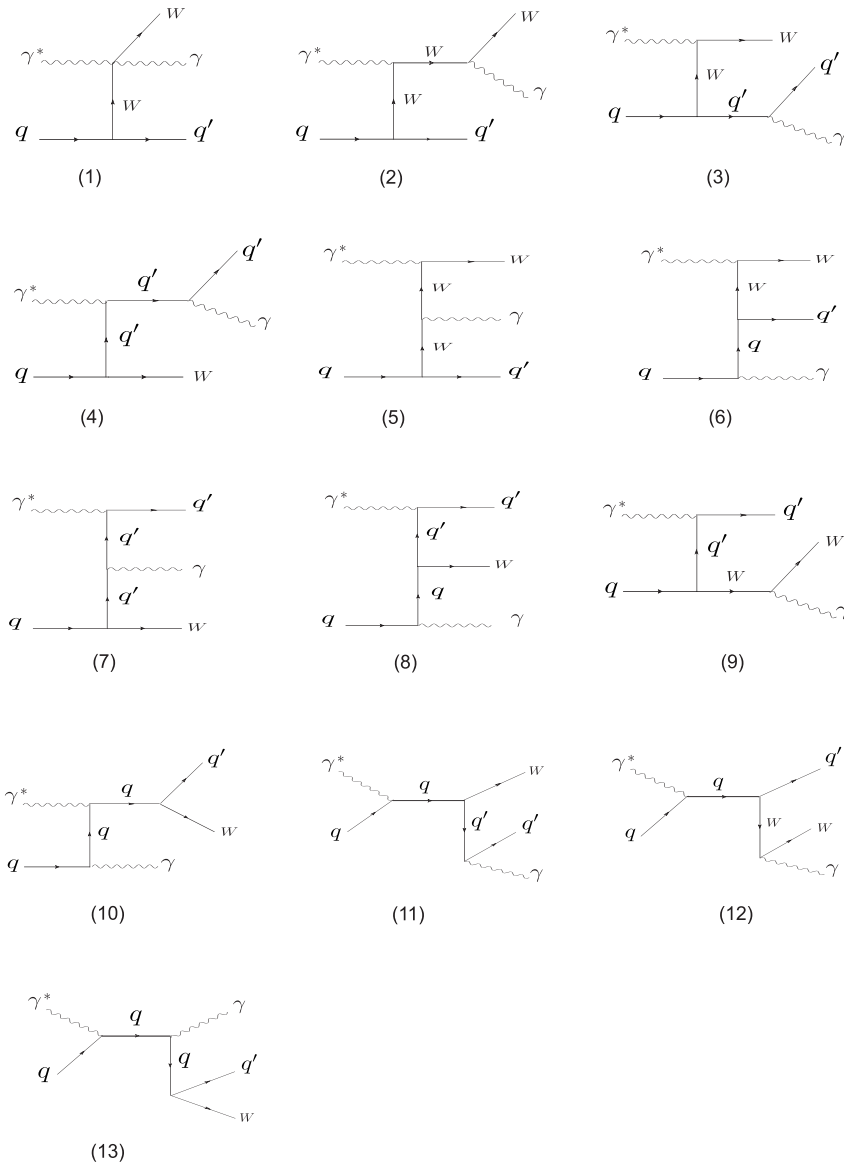


FIG. 2: Feynman diagrams contributing to the subprocess  $\gamma^* q \rightarrow W \gamma q'$ .



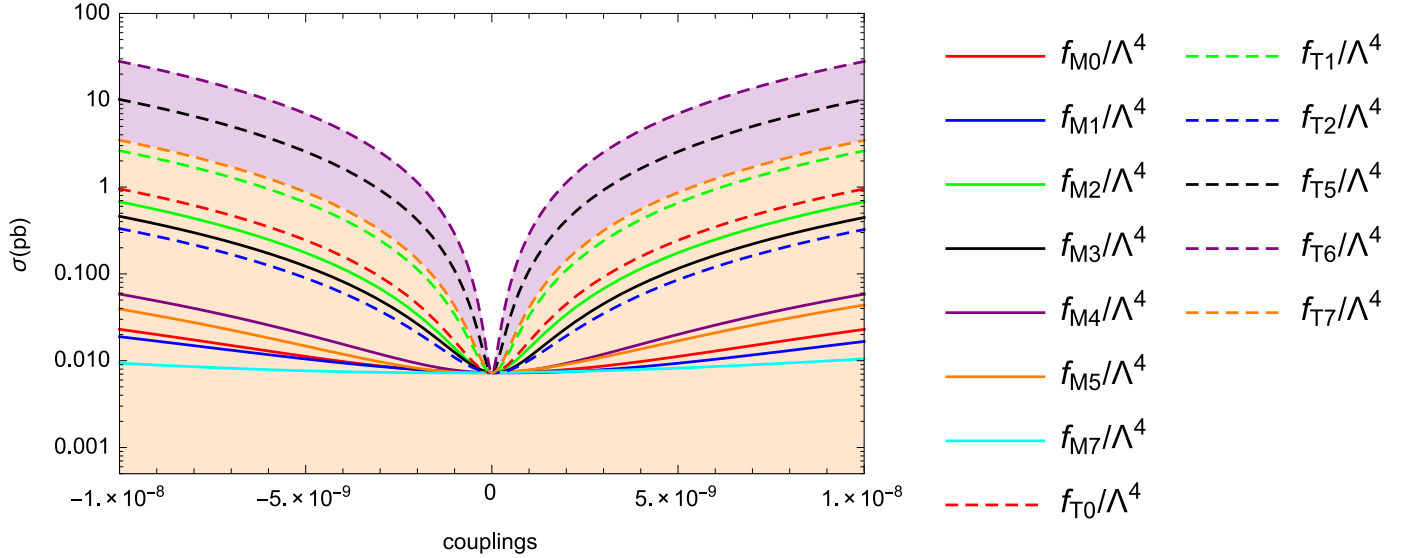


FIG. 3: For pure-leptonic channel, the total cross sections of the process  $e^-p \rightarrow e^- \gamma^* p \rightarrow e^- W^+ \gamma q X$  as a function of the anomalous couplings for center-of-mass energy of  $\sqrt{s} = 1.30$  TeV at the LHeC.

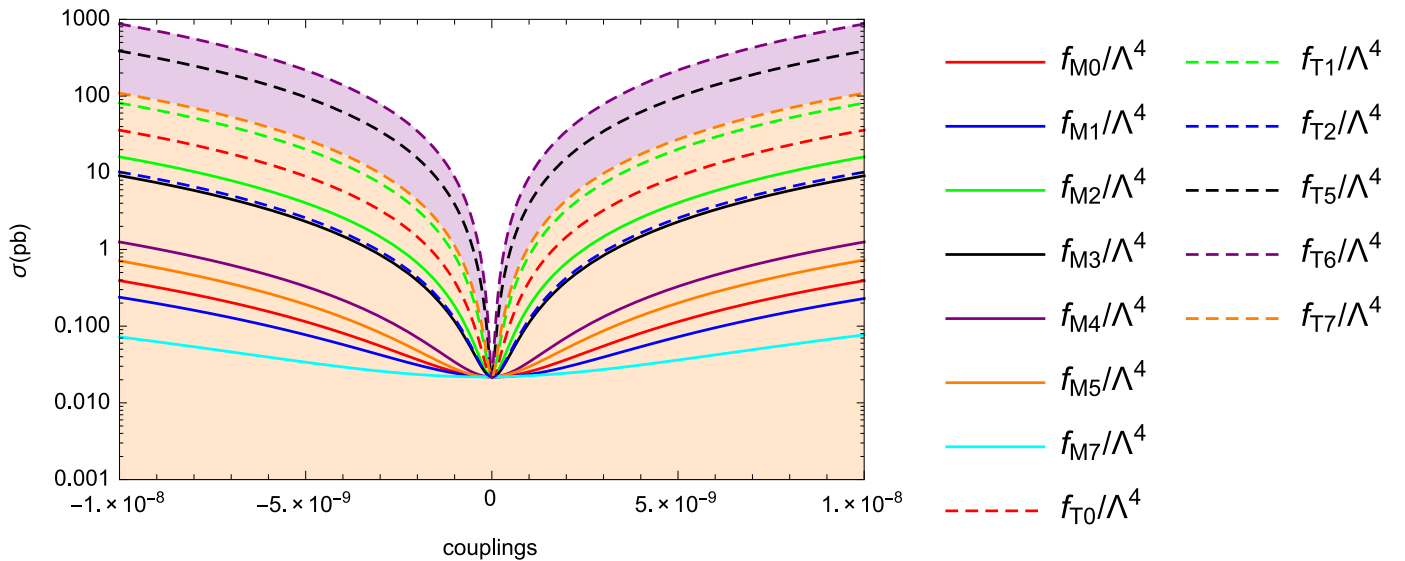


FIG. 4: Same as in Fig. 3, but for  $\sqrt{s} = 1.98$  TeV at the LHeC.

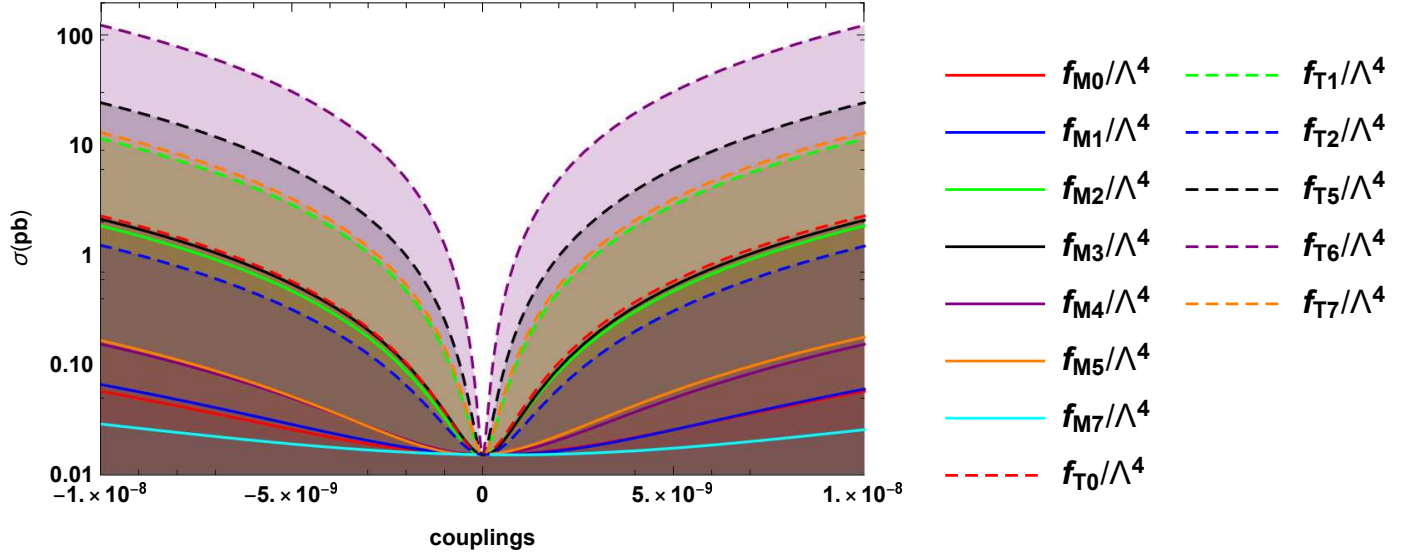


FIG. 5: Same as in Fig. 3, but for hadronic decay.

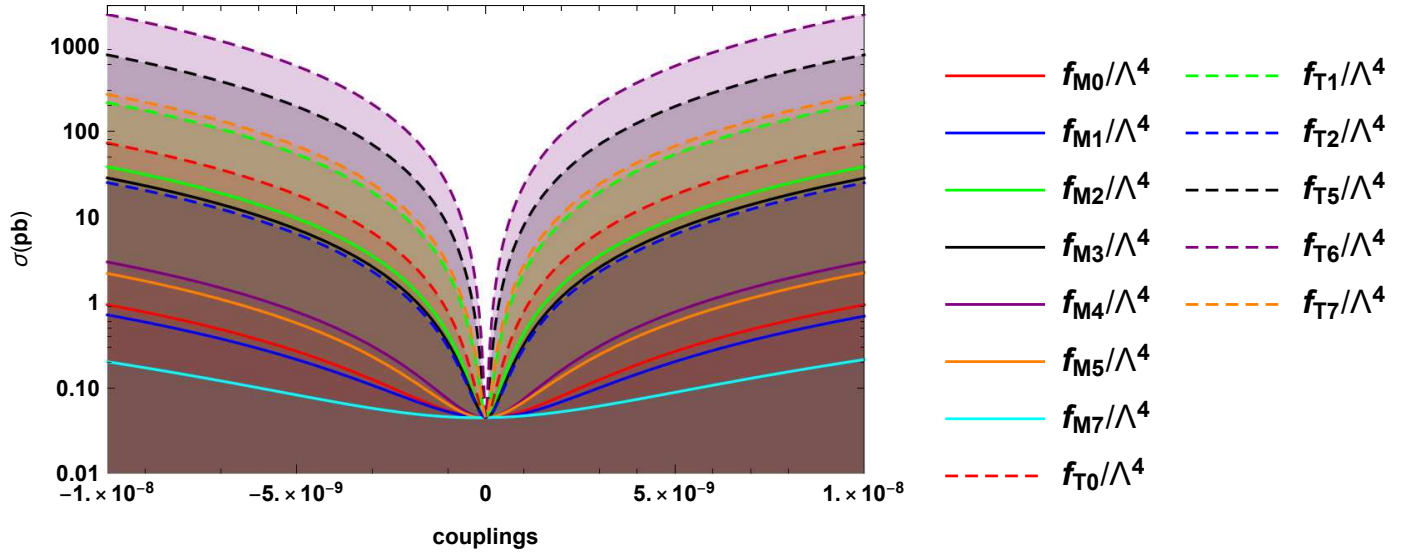


FIG. 6: Same as in Fig. 4, but for hadronic decay.

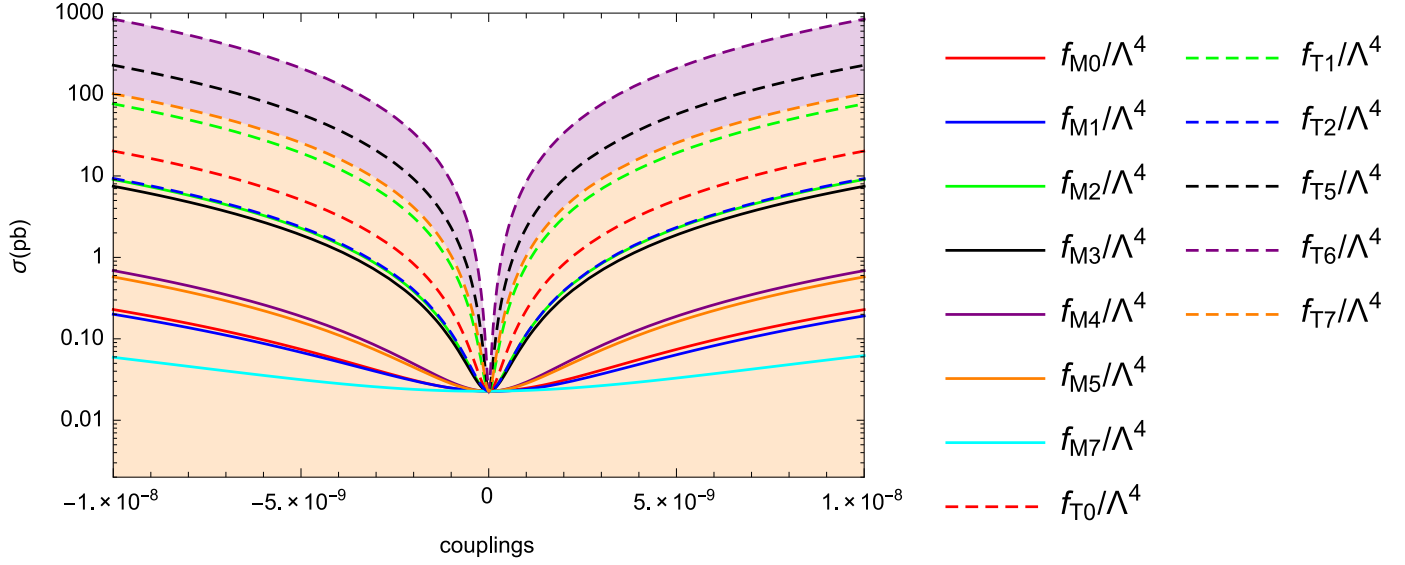


FIG. 7: For pure-leptonic channel, the total cross sections of the process  $e^-p \rightarrow e^- \gamma^* p \rightarrow e^- W^+ \gamma q X$  as a function of the anomalous couplings for center-of-mass energy of  $\sqrt{s} = 3.46$  TeV at the FCC-he.

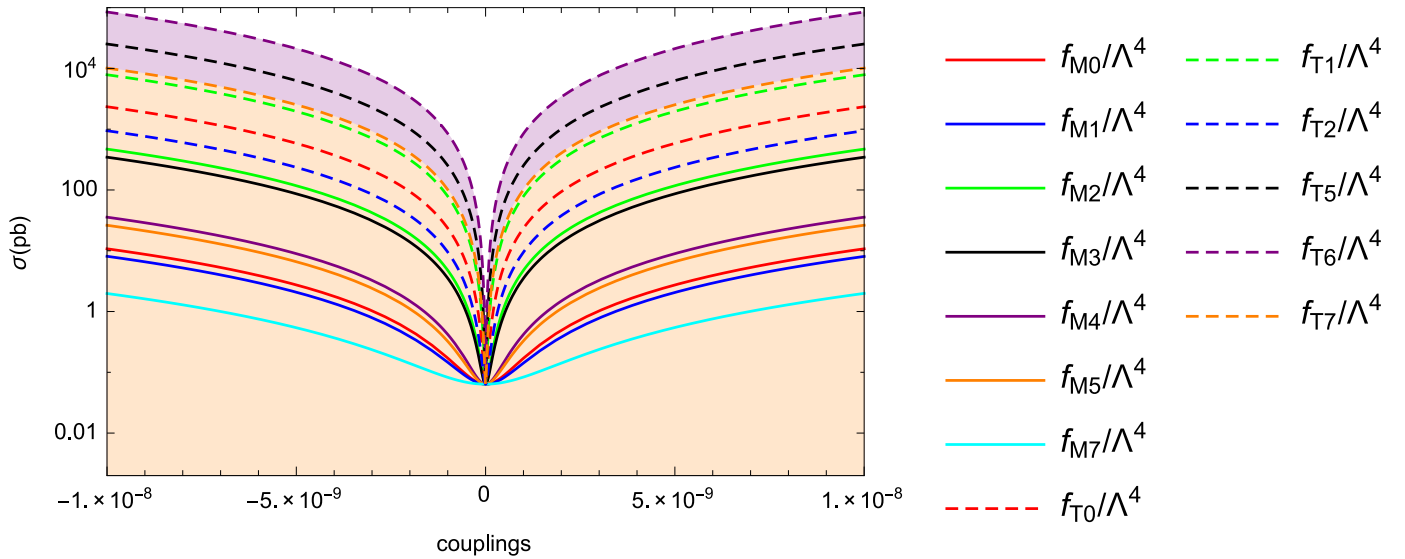


FIG. 8: Same as in Fig. 7, but for  $\sqrt{s} = 5.29$  TeV at the FCC-he.

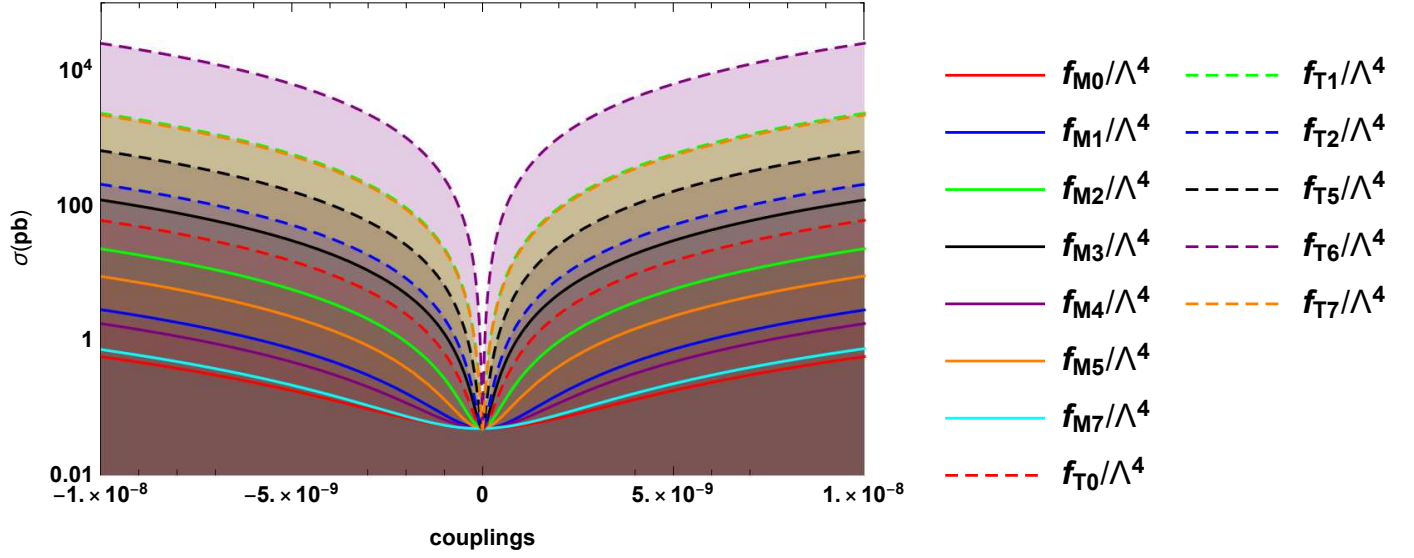


FIG. 9: Same as in Fig. 7, but for hadronic decay.

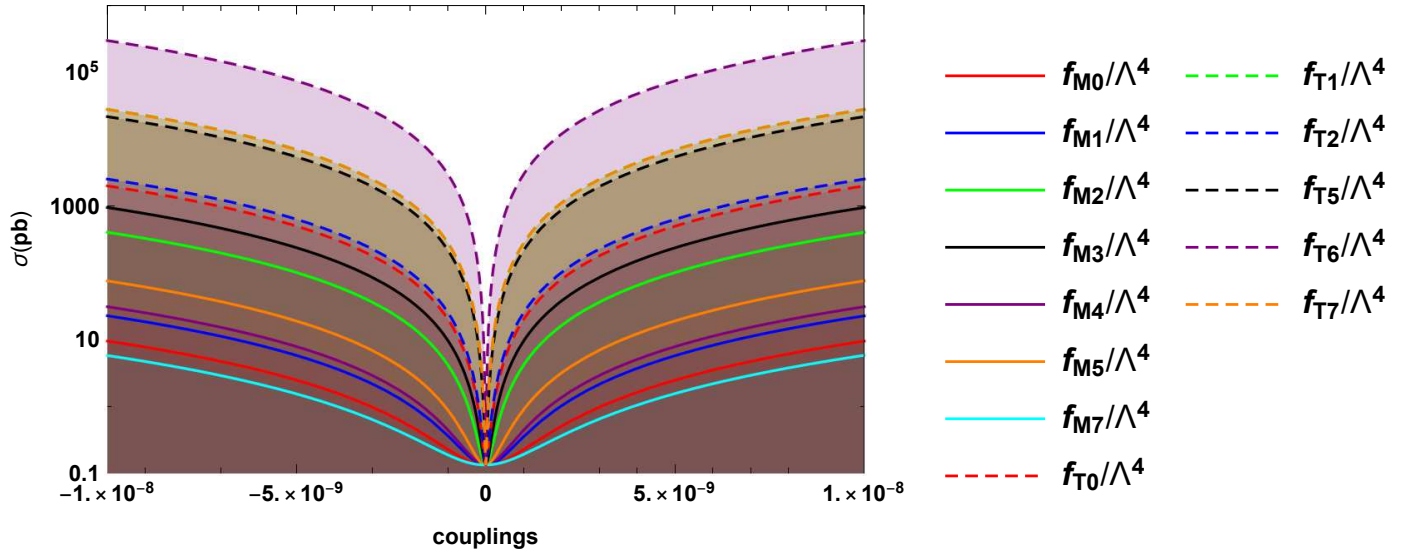


FIG. 10: Same as in Fig. 8, but for hadronic decay.